Manuscript Details

Manuscript number	VIBSPEC_2018_247_R1
Title	Combined vibrational, structural, elemental and Mössbauer spectroscopic analysis of natural phillipsite (zeolite) from historical eruptions in Tenerife, Canary Islands: Implication for Mars
Article type	Research Paper

Abstract

The outcrop of “Las Arenas” volcano in Tenerife, Canary Islands (Spain) has been presented as Terrestrial volcanic analog for ancient Mars, showing a great variety of alteration processes and interesting mineralogy. The current analysis has been done by means of measurement techniques used or proposed on Martian studies. The new analysis of the zeolite has been carried out using Raman spectroscopy, Mössbauer spectroscopy, X-ray diffraction (XRD), Infrared spectroscopy, Laser induced breakdown spectroscopy and Scanning electron microscopy (SEM-EDX). The zeolite has been mainly carefully analyzed using vibrational spectroscopy and it has been identified as Ca-phillipsite. The other techniques support and confirm the results. The measurements and results using the Raman Laser Spectrometer (RLS) simulator system show the capabilities RLS system in the ESA Exo-Mars mission. The chemometrical methods for the vibrational mineral detection show the advantages of Raman spectroscopy to understand the possible geological context. Furthermore, the proposed diagenesis and formation of the zeolites in southern part of Tenerife island have been confirmed by the twin space prototypes used. Furthermore, a new hypothesis about the origin for the special case of “Las Arenas” volcano Ca-phillipsite has been proposed. Finally, a multi-complementary comparison among the different techniques used on the current studies has been done and, also an analogy with the next space mission has been established. These analyses emphasize the strength of the different techniques and the working synergy of the different techniques together for planetary space missions.

Keywords	Vibrational spectroscopy; Phillipsite; Planetary science; Raman spectroscopy;

Corresponding Author	Emmanuel Lalla
Corresponding Author's Institution	Centre for research of earth and space science, York University
Order of Authors	Emmanuel Lalla, Guillermo Lopez-Reyes, Antonio Lozano-Gorrín, Fernando Rull

Suggested reviewers	M Hipondoka, Márta Polgári, Pieter B. Kotzé, Abdelwaheb Inoubli

Submission Files Included in this PDF

File Name [File Type]

Cover Letter.pdf [Cover Letter]

Answer to reviewers.docx [Response to Reviewers]

Manuscript_final.docx [Revised Manuscript with Changes Marked]

Highlights_final.docx [Highlights]

Manuscript.docx [Manuscript File]

List of Figure_final.docx [Figure]

Figure1.tif [Figure]

Figure2.tif [Figure]

Figure3.tif [Figure]

Figure4.tif [Figure]

Figure5.tif [Figure]

Figure6.tif [Figure]

Figure7.tif [Figure]

Figure8.tif [Figure]

Figure9.tif [Figure]

List of Table_final.docx [Table]

Supporting Material_final.docx [Supplementary Material]

To view all the submission files, including those not included in the PDF, click on the manuscript title on your EVISE Homepage, then click 'Download zip file'.

Research Data Related to this Submission

There are no linked research data sets for this submission. The following reason is given:
Data will be made available on request

This is the preprint version of the following article: Vibrational Spectroscopy, 2019. vol. 101, p. 10–19, which has been published in final form at: https://doi.org/10.1016/j.vibspec.2018.12.003

Combined vibrational, structural, elemental and Mössbauer spectroscopic analysis of natural phillipsite (zeolite) from historical eruptions in Tenerife, Canary Islands: Implication for Mars

E. A. Lalla[1,2,*], G. Lopez-Reyes[3], A.D. Lozano-Gorrín[4,5] and F. Rull[3]

[1] Centre for research in earth and space science, York University, Petrie Science Building, 4700 Keele St, Toronto, M3J 1P3, Ontario, Canada.

[2] Austrian Space Forum, Sillufer 3a, Innsbruck, 6020, Austria.

[3] Unidad Asociada UVa-CSIC al Centro de Astrobiología, Parque Tecnológico de Boecillo, Valladolid, Spain.

[4] Departamento de Química, Universidad de La Laguna. Avenida Astrofísico Francisco Sánchez, s/n. 38200 La Laguna, Tenerife, Spain.

[5] Instituto Universitario de Materiales y Nanotecnología. Universidad de La Laguna. Avenida Astrofísico Francisco Sánchez, s/n. 38200 La Laguna, Tenerife, Spain.

Abstract

The outcrop of "Las Arenas" volcano in Tenerife, Canary Islands (Spain) has been presented as Terrestrial volcanic analog for ancient Mars, showing a great variety of alteration processes and interesting mineralogy. The current analysis has been done by means of measurement techniques used or proposed on Martian studies. The new analysis of the zeolite has been carried out using Raman spectroscopy, Mössbauer spectroscopy, X-ray diffraction (XRD), Infrared spectroscopy, Laser induced breakdown spectroscopy and Scanning electron microscopy (SEM-EDX). The zeolite has been mainly carefully analyzed using vibrational spectroscopy and it has been identified as Ca-phillipsite. The other techniques support and confirm the results. The measurements and results using the Raman Laser Spectrometer (RLS) simulator system show the capabilities RLS system in the ESA Exo-Mars mission. The chemometrical methods for the vibrational mineral detection show the advantages of Raman spectroscopy to understand the possible geological context. Furthermore, the proposed diagenesis and formation of the zeolites in southern part of Tenerife island have been confirmed by the twin space prototypes used. Furthermore, a new hypothesis about the origin for the special case of "Las Arenas" volcano Ca-phillipsite has been proposed. Finally, a multi-complementary comparison among the different techniques used on the current studies has been done and, also an analogy with the next space mission has been established. These analyses emphasize the strength of the different techniques and the working synergy of the different techniques together for planetary space missions.

Keywords: Vibrational spectroscopy; phillipsite; planetary science; Raman spectroscopy.

Introduction

The volcanic activity of the island of Tenerife has been studied due to the interesting results it brings when it comes to volcanic prediction, geological evolution of Earth, geochemistry, etc. In fact, the historical eruptions are of special interest since the characterization of the natural samples and the mineral species allows scientists to obtain and elucidate accurate results of the past of Mars [1–3]. In the case of the Canary Islands, the main advantage of the historical eruptions is that they have been well documented throughout history. Among the most important historical eruptions that took place in Tenerife, it is important to mention: (1) the triple fissure Fasnia, Siete Fuentes and volcano of Las Arenas (in 1704 and 1705) [4] , (2) the eruption of Montaña Negra in Garachico (in 1706), (3) the volcano of Pico Viejo, Chahorra (in 1798) [5] and the volcano of Chinyero (in 1909) [6].

The volcanoes of Fasnia, Siete Fuentes, Las Arenas and Chinyero are located in the southeastern part of the island where the occurrence of zeolites in the pyroclastic and basaltic deposits has been documented [7]. Furthermore, the geologic conditions are very favorable for some specific zeolite formations. Among the most important reported minerals are phillipsite, chabazite and analcime, being the phillipsite the most abundant from the previous studies. Furthermore, García-Hernández et al. (1993) concluded that the zeolites were formed by the action of water vapor trapped within the pores of the volcanic glasses [7]. In this sense, the high temperature and closed system conditions create favorable rapid method to nucleate and grow zeolite from water vapor and volcanic glass [8].

Special consideration should be taken into account about the zeolites in the Martian environments; it has been suggested that these minerals could have strong impact in the

Martian environment and atmosphere [9]. There exists the possibility that zeolites could be a reservoir system of the methane in the Martian subsurface [10]. Furthermore, another recent hypothesis suggests that the zeolite distribution could be present in certain dust-poor regions affecting the diurnal atmospheric water cycle along the seasons [11,12].

On this research, a complete analysis of zeolite detected in certain samples from the volcano of Las Arenas using a complete combination of present and future space instrumentation for planetary science focused on Mars is presented. The volcanic outcrop has been already proposed as possible terrestrial analog for the ExoMars Mission and it has been fully analyzed by means of Raman spectroscopy to complement the science behind the Raman Laser Spectrometer (RLS). However, a detailed analysis of certain secondary mineralization detected on these samples has not been done yet using techniques already or about to be applied in Martian Rover missions. The detailed analysis has been carried out by Raman spectroscopy, Laser induced breakdown spectroscopy and X-ray diffraction (XRD) working in synergy using certain twin prototype instruments such RLS-simulator and Terra-Insitu XRD. In addition, SEM-EDX microscopy and Infrared spectroscopy have helped to strongly complement the results and characterize the zeolite detected.

Experimental results and sampling methods

The sample set was collected by picking out samples on the studied areas on expeditions to the Canary Islands in 2010, being all of them catalogued and photographed. The detailed pictures of the samples have been documented and the detailed mineralization is presented on E. Lalla et al. (2015) [13]. The main minerals detected on the outcrop are summarized on the supplementary section (See Table S-1). The SEM-EDS measurements were obtained by

using a Scanning Electron Microscope FEI - Quanta 200FEG. The system is equipped with electron cannon emission type with Schottky filaments using an acceleration voltage of 30 kV with EDS Oxford Inca Energy 350, equipped with secondary electron detectors. For this analysis, no sample preparation was necessary and the measurements were directly performed on the bulk samples.

The images of the different vesicles studied were obtained by Nikon SMZ 800 stereo-microscope system illuminated with a LED flashlight system. The system is equipped with a Nikon standard eyepiece C-W 10X and an objective lens APO 1X. The zoom range for the current system is from 1X up to 10X approximately. The images were obtained at 10X magnification with a field of view of 2.8 mm.

The XRD patterns were obtained with a Terra XRD-diffractometer instrument based on the MSLCheMin concept with a 1024x256 detector working in 2D-CCD mode. The XRD source was obtained by a cobalt X-ray tube of 30 KV-300 mA. The preparation consisted on the powdering of a minimum part of the samples (2−4 mg) and sieved with a granulometry lower than 150 mm. The analysis and identification was done using the software from Terra-In-Situ XPowder by pattern matching with the JCPDS database and manually double checked with the XRD diffractogram from RRUFF and using Crystal Sleuth [14,15].

The micro-Raman measurement of the samples was performed with a microscope Nikon Eclipse E600 coupled to a spectrometer KOSI Holospec f/1.8i, with best spectral resolution of 5 cm^{-1}, illuminated by a laser REO LSRP-3501 He-Ne (632.8 nm wavelength). The detection was performed by a CCD Andor DV420A-OE-130. The laser power used on the sample was 14 mW with a minimum spot diameter of 15 µm. The Raman mapping of the

bulk surface of the sample was done with a Micro-Raman Prior Proscan II motorized stage in automatic mode in order to detect the different compositional mineralization. The RLS Raman automatic measurement were done by the ExoMars RLS Simulator in automatic mode acquiring several spectra per sample, with automatically calculated integration time and number of accumulations at each point [16]. The laser wavelength corresponds to 532 nm with a spot size of 50 microns and irradiances of 0.25 and 1 kW/cm^2 [16,17].

The FT-Raman analysis was performed with a Fourier Transform Raman (FT-Raman) Bruker RSF 100/S, which allows the analysis of high fluorescence samples, making it more suitable for some samples than the visible Raman equipment. The FT-Raman spectrometer is composed of a Nd:YAG Laser at 1064 nm, with spectral range 851−1695 nm (NIR) and best spectral resolution of 2 cm^{-1}. The detector is a Bruker CCD model D418T cooled by liquid N_2. The working conditions achieved a spectral resolution of 4 cm^{-1} and a diameter spot of 100 mm approximately.

Fort the LIBS measurements, the system used was a StellarNet PORTA-LIBS 2000 with a spectral range from 400 to 850 nm. The excitation source was 1064 nm Nd:YAG laser with a pulse duration of 6 ns and a total energy of 1 GW cm^{-2} onto the spot.

The results were directly measured from the fresh part sample material without any sample preparation. The spectroscopic analysis was done processed by means of a Gaussian curve fitting in order to determine the correct band position, intensity, FWHM and spectral profile for the different mineral phases detected. We used a Bruker OPUS to calculate the fitting on the sample and following the standard procedure available on the software such as spectra smoothing (whenever is required), background subtraction, normalization and Levenberg-

Marquardt curve fitting. The mineral identification has been done according the RRUFF database, Romanian Raman Database and other references that will be included in the discussion section [14,18].

The Mössbauer spectra were collected with a copy of the MIMOS II spectrometer from the past NASA-MER-mission (AK Klingelhoefer, Mars Mössbauer Group, Mainz, Germany). The system has a Co^{57}/Rh source with an intensity of about 50 mCi. The measurements have been performed at room temperature and without sample preparation in a backscattering geometry. The method of analysis was the same as C. Markowski et al., (2017) and E. Lalla et al., (2016) [2,19,20].

Analytical results

Figure 1 shows an example of the vesicles where the zeolites have been detected from previous studies.

Raman Spectroscopy Analysis

The phillipsite minerals with the chemical formula $(Ca,Na_2,K_2)_3Al_6Si_{10}O_{32}\cdot 12H_2O$ crystalize in a monoclinic system with the space group $P\ 2_1/m$ [21]. Indeed, it has been reported that the crystal lattice of this zeolite is mainly formed by interconnected long chains of (Al, Si)O_4 tetrahedra. Every single chain is a subsequently combination of four tetrahedral and the water molecules and/or cations are localized in the channels formed between the principal and secondary chains [21]. The theoretical factor group analysis already calculated from the reference has [21]:

$$T_{Opt} = 147A_1(IR,R) + 146A_2(R) + 146B_1(IR,R) + 146B_2(IR,R) \quad (1)$$

Where the symmetric modes A_1, B_1 and B_2 are active in the spectra for both Raman and Infrared modes. In this sense, the Raman spectrum is a combination of the longitudinal ad transverse vibrational modes (LO and TO) [21]. Also, it has to be considered that it is not possible to separate the LO and TO modes due to the fact that these modes could be degenerated. However, F. Pechar et al (1981) presented the experimental vibrational results and it all can be divided in the main factor groups [21]: (1) the optical modes of the crystal lattice (from 50 to 600 cm^{-1}); (2) the internal vibrations of the water molecules (from 1600 to 3700 cm^{-1}); (3) the internal vibrations of the bonds from the Al/Si-O_4 (from 400 to 1000 cm^{-1}); and (4) the external vibrations of H_2O molecules (from 300 to 680 cm^{-1}).

On the other hand, S. Goryainov and M Smirnov et al (2001) presented a similar study on Natrolite (zeolites) under different pressure conditions [22]. In their research the group theory of active modes corresponds to Eq.(2):

$$T_{Opt} = 24A_1(IR,R) + 25A_2(R) + 25B_1(IR,R) + 25B_2(IR,R) \qquad (2)$$

where all the Raman are under 1000 cm^{-1}, and also from the 99 optically active modes 36 are experimental optically active in Raman and Infrared spectroscopy. Besides, as F. Pechar et al (1981) predicted, the vibrations are water molecules, OH^- and a combination of the longitudinal ad transverse vibrational modes (LO and TO) [22].

Table 1 compiles Gaussian fitting position from some spectra obtained from the Micro-Raman analysis with the complementary theoretical assignment from F. Pechar et al (1981) and S. Goryainov and M. Smirnov et al (2001) [21,22]. Also, the spectra from other phillipsite minerals from RRUFF like Ca-phillipsite (R050078), K-phillipsite (R140774) and Na-phillipsite (R061094) are included for comparison [14]. Figure 2 shows the different

spectra from Table 2 and the graphical band assignment. A similar analysis was carried out using the spectra obtained by the ESA-ExoMars RLS simulator. The samples were automatically aligned, and best exposure and acquisition were automatically calculated from the RLS software. The band positions from Gaussian fitting of the Raman bands are listed in Table 2 and Figure 3 shows the spectra from the same spot analyzed in Figure 1.

Infrared Spectroscopy Analysis

Following the Eq. (1), the IR spectrum of the phillipsite presents the following IR active modes and they can be assigned as: (1) asymmetric stretching vibration of the bridge bonds ν_{asym}(Si-O-Si) and ν_{asym}(Si-O,Al) at ~1000 cm^{-1}; (2) the symmetric stretching vibrations of the bridge bonds ν_{sym}(Si-O-Si) at ~720 cm^{-1}, (3) the symmetric stretching vibrations of the bridge bonds ν_{sym}(Si-O-Al) at ~670 cm^{-1}, (4) the complex band from the combined symmetric stretching vibrations ν_{symm} (Si-O-Si) and bending vibrations – δ(O-Si-O) at ~550 cm^{-1}, (5) the bending vibrations δ(O-Si-O), occurring in 468 cm^{-1} and (6) the bending vibrations δ (O-Si-O)/δ(O-Al-O) around 377 cm^{-1} [21–23]. Also, the zeolite uses to present the external vibrations of H_2O molecules created by the hydration. Among the most intense, H_2O at ~3300 cm^{-1}, asymmetric vibrations of (O-H) at 3600 cm^{-1} and the (Al,Si)-OH vibrations around 1650 cm^{-1} can be observed. The supporting material summarizes all the principal assigned Infrared bands detected in Las Arenas volcano´s phillipsite and a comparison with the IR spectra available at RRUFF has been done (standard selected: Na-phillipsite (R061094), K-phillipsite (R140774), Ca-phillipsite (R050078)) [14,23] (see Table S-2). Figure 4 compiles the Gaussian fitting analysis from Table 3 containing the IR spectrum of phillipsite, the other points present similar behavior. On the other hand, the comparison with a Na-phillipsite (Sif Z99) from N. V. Chukanov (2014) shows a similar behavior [24].

It has been observed that main intense band (ν_{asym}(Si-O-Si) and ν_{asym}(Si-O,Al)) is lightly shifted to higher values around 1000 cm^{-1}, however the band position of ν_{sym}(Si-O-Al) is more or less in a pretty similar position. The bands related to ν(Al,Si)-OH at ~1630 cm^{-1} and ν_{assym}(O-H) / H_2O present quite similar positions in both spectra (Na-phillipsite and Las Arenas Negras volcano phillipsite) [23–25].

Scanning Electron Microscopy

The Scanning Electron Microscopy analysis in Figure 5 shows the existence of the phillipsite that can be confirmed by pseudo-orthorhombic structure with an elongation along b axis. The points (c) and point (d) present similar structures as the points (a) and (b). Thus, no significant difference in shape and size was observed among the different samples of different outcrops. The formation of the phillipsite inside de vesicles of the bulk matrix is accordance with other similar results occurring in radiating clusters [7,26]. On the other hand, the SEM also shows the occurrence of other crystal formation such as the calcite. Taking into consideration the crystal Atlas, calcite can be observed by observing the different trigonal structures with a point group 32/m. Calcite shows to be coarse grained and possibly cement-filling central parts of vesicles and the inter-granular spaces. The chemical analyses of the phillipsite from the different sample point are reported in supporting material (see Table S-3).

Laser Induced Breakdown Spectroscopy (LIBS)

LIBS data were acquired in the visible range (from blue & violet, visible and near infrared wavelengths) on the point (d) (see Figure 1) and it is summarized in Figure 6. The identification of the peaks were done using the NIST LIBS library and Figure 6 only illustrates the most of the major elements detectable over these wavelength ranges [27]. The

elements identified in the LIBS spectra are Fe, Si, Al, Ca, K, O, Mg, C and Na. The elements detected match with the elemental composition of the general stoichiometry of the phillipsite in combination with the calcite. Furthermore, a small variability concerning the peak intensities has been found, being an indicator of changes in the elemental abundance. The most notable variability corresponds to the ones assigned to C, O and Ca, which could be related to the abundance of calcite in the different vesicles and/or laser spot used for measurements. The elements detected match and they can be confirmed by the SEM-EDS results in (see Table S-3). However, some elements, like Ti and P, were not detected due to resolution of the spectrometer and laser power (to create plasma on Ti/P).

X-Ray Diffraction/X-Ray fluorescence

The mineralogy obtained by the XRD in one of the samples shows the detection of the phillipsite and calcite in the diffraction pattern. Figure 7 presents the mineral identification with the standard RRUFF samples (Ca-phillipsite (R050078), K-phillipsite (R140774) and Na-phillipsite (R061094) for a better appreciation of the phillipsite detection [14]. However, there is also other minerals quartz, feldspar, clays (detected and not patterned), olivine and pyroxenes due to the extraction. The extraction method was done by carefully scratching the minerals (phillipsite and calcite) from one of the vesicle. Thus, the vesicle minerals also contain the bulk main mineralization from samples which can be confirmed from Table 1 and from previous results in E. Lalla et al (2015) [13]. On the other hand, the confirmation of the existence of the Ca-phillipsite has been checked by two other methods: (1) comparison with the XRD diffraction pattern from standard RRUFF samples (a) Na-phillipsite (R061094), (b) K-phillipsite (R140774), (c) Ca-phillipsite (R050078) [14] and also (2) by comparing the XRD results presented on J. E. Garcia Hernandez [7].

The Terra Insitu XRD is capable to obtain also X-ray fluorescence measurements. The results obtained are shown in Figure 8, where the elements detected by internal analysis of the instrument shows the detection of Ca, Si, Al, Ti, Fe, and K that correspond to the elements that form part of the minerals and they match with LIBS elemental identification and SEM-EDX elemental identification-quantification. However, there are some limitations on the XRF system from the Terra Insitu to be considered due to the fact that the XRF mode system was designed as a support method to complement the XRD [28,29]. Thus, XRF is a semi-quantitative elemental analytical system to enforce the XRD mode. First of all, there is a reduced sensitivity below Si transitions due to Be window and chip technology used on the system. Also, the Co from the source used caused high intense diffracted peaks masking others. Finally there also exists an over estimation of Fe, Mn and Cr due to the contamination from the CCD housing and stainless steel of the structure [29].

Mössbauer Analysis

Mössbauer spectroscopy analysis has been performed measuring some selected samples where the phillipsite was visually observed from E. Lalla et al (2015) and E. Lalla et al (2010) [4,13]. The hyperfine parameter (as isomer shift (IS), quadrupole splitting (QS) and spectral line width) and the corresponding minerals detected, derived from the data, are listed in Table 6 and shown in Figure 9. The different sub-spectral areas obtained by a band fitting from the different samples show Fe-content minerals only following the methods in the references [2,19,20] and the standard used for comparison were from [30,31]. The results showing the presence of olivine, pyroxene, magnetite, goethite, and oxide phase with different degrees of crystallinity have been also confirmed on E. Lalla et al (2015) [4,13].

Discussion

The vibrational analysis from the theoretical perspective using the group theory has been confirmed using the experimental results and carefully analyzed with a Gaussian profile fitting. During the analysis, it has been compared with several standards Raman from RRUFF using the 3 different phillipsitic kind such Ca, Na and K- phillipsite. By taking into consideration the Raman band profiling, the phillipsite corresponds to a Ca-phillipsite by the match of the ν_{symm}(O-(Al,Si)-O) at 419, ν_{int} (Al,SiO_4) at 480 and ν_{int} (Al,SiO_4) at 505 cm^{-1} [21]. However, Pechar et al (1981) did not assigned to which of the internal vibration belong. In these sense, from recent results, these vibrations could certainly be assigned to a combination of O-T-O symmetric bending breathing vibrational mode, O-T-O bending bending mode and librational modes of the water [22]. The subsequent confirmation was carried out by the RLS simulator of same Raman vibrations and detection of other bands like ν_{symm}(Al,Si)-O at ~760 cm^{-1} . Furthermore, the RLS system has shown more sensitivity and water and OH^- related vibrations bands at ~120-140 cm^{-1}, ~1630 cm^{-1} and ~3500-3600 cm^{-1} have been also detected (see Tables 2 and 3). On the other hand, the ν_{assym}(Al,Si)-O Raman bands, located between 1000 and 1150 cm^{-1}, were observed on the Raman spectra from the RRUFF standards. These modes could correspond to the T-O asymmetric stretching among in Si_2O_4 and AlO_4 considering other similar zeolite type [21,22]. However, the same bands in our samples were not detected due to the fact of having low intensity peak value and they were masked by the intense band of the calcite, high-content of magnesium calcite and/or minor concentration of dolomite. The carbonates detected present the most intensive vibrations on: (1) the 1080-1100 cm^{-1} range which correspond to the symmetric stretching of the CO_3; (2) symmetric bending of the CO_3 between 700 and 720 cm^{-1} and (3) the external

vibration of the CO_3 at around 280 to 290 cm^{-1} [32,33]. In our case, the carbonate detected corresponds to the existence of calcite with the main vibration band at ~1087 cm^{-1}. The shoulder band detected from ~1090 to ~1100 cm^{-1} could correspond to the mineral phases such dolomite or a high magnesium content carbonate [33].

The technique based on vibrational spectroscopy like the Infrared spectroscopy also matched with Ca-phillipsite mineral type. The main confirmation has been done by the ν_{sym}(Si-O-Al) at ~670, ν_{sym}(Si-O-Si) at ~730 and the ν_{asym}(Si-O-Si)/ν_{asym}(Si-O,Al) at ~989 cm^{-1}. Also, the water vibration predicted by Pechar et al. (1981) [21] was measured being at ~1638 (ν(Al,Si)-OH), ~3200 (ν(H_2O) and ~3400-3600 (ν_{assym} (O-H)) cm^{-1}. The calcite was detected on the spectra and it is presented in Figure 4. Furthermore, the Infrared spectroscopy shows that most intense bands were not overlapping the other bands from Las Arenas volcano Ca-phillipsite.

The elemental composition analysis carried out by the portable instrumentation like LIBS and XRF were in agreement with the detection of iron (Fe), potassium (K), sodium (Na), magnesium (Mg), aluminum (Al), silicon (Si), carbon (C), oxygen (O) and calcium (Ca). Concerning both techniques, LIBS shows more sensitivity to the elements given the limitation of the XRF mode of the Terra-Insitu aforementioned. However, in both analyses, Ca has been commonly detected as the major compared to Na or K by comparing the intensity, helping to confirm calcic nature of the mineral from the vibrational analysis (Raman-IR). Furthermore, the C element on both techniques has been detected, which could correspond to the calcite detected on the samples. The SEM-EDS confirmed and determined the elemental compositions of the different vesicles measured by LIBS and XRF. In the different points (a), (b) and (d), the results show a similar behavior with the exception of the

vesicle (c) where it can have a bigger concentration of calcite given the high values of CO. Taking into account the Si/Al ratio, it has been observed that phillipsite from Las Arenas volcano presents the following values: (a) 2.18, (b) 2.20, (c) 2.12, and (d) 1.95. The current values match with the results from previous studies, where the general trend is from 2.00 to 2.15 approximately [7]. In the special case of the Las Arenas volcano, phillipsite, compared to the other zeolites detected in the south of Tenerife, presents higher values of Ca concentration.

The XRD results showed the presence of the phillipsite in the presence of the bulk matrix rock forming minerals like feldspars, pyroxenes, olivines and quartz. In Figure 7, the analysis of the extracted powdered from one vesicle and compared with the RRUFF XRD standards is shown. It can be observed that the presence of the principal peaks may be masked with other more active minerals for XRD given the crystallinity and crystal orientation during the measurement. The principal values presented in J. E. Garcia Hernandez et al (1993) [7] match with the results obtained in the present research. Also, J. E. Garcia Hernandez et al (1993) has discussed that Tenerife´s phillipsites are quite different from others (such as Italian phillipsites presented on [7]) due to the fact that the mineral presents lower values for the c-axis and, therefore, smaller unit-cell volumes [7].

Finally, the Mössbauer analysis carried out at Mainz University showed the detection of the principal rock forming minerals from the matrix. Among the main minerals detected, one can find olivine, pyroxene, amorphous phases of Fe_2O_3 and magnetite.

In previous results, J. E. Garcia-Hernandez et al (1993) presented Tenerife phillipsites as an intermediate between the diagenetic and the deep-sea ones [7]. Phillipsites from deep-sea

sediments and saline lake deposits have larger Si/Al ratios, which is not the case of Las Arenas volcano. The sequence of occurrence and paragenesis found out is the following: Glass → Phillipsite → Phillipsite + Analcime → Phillipsite + Analcime + Feldspar [7,13]. Furthermore, the hypothesis about origin of zeolite kind could be confirmed by the Raman-IR spectroscopy, where the water vapor trapped interact with the glass particles by hydrothermalism promoting the formation of zeolites [7]. Thus, the water vapor in contact with the melting volcanic glass in closed-system conditions promotes the glass hydration, with a subsequent dissolution and nucleation. Finally, when the temperature starts to decrease, the growth of zeolite crystals can be originated [7,26]. Nonetheless, in the special case of Las Arenas volcano and according with the current measurements, the phillipsite is a Ca-enriched solid solution. The origin could probably happen by a direct formation in Ca-bearing solutions or by post-zeolitization cation exchange among the Ca, Na and K. Finally the formation of the accessory calcite could be related to CO_2 gases in combination with H_2O providing hydrolysis reactions [34]. The carbonate ions (CO_3^{2-}) could be combined with excess of Ca and started to form calcite. The detection of calcite by Raman-IR spectroscopy and XRD/XRF and LIBS confirms the enrichment of Ca in the phillipsite and calcite suggesting a low CO_2 fugacity during the zeolitization process. However, more detailed studies to support this idea from the data presented in this research will be needed and it must be regarded as a hypothesis.

The vibrational spectroscopic analysis, like Raman and Infrared, is a powerful tool giving new perspectives and viewpoint of the ideas as well as complement about the paleogenesis of the Ca-phillipsite of Las Arenas. However, a conjunction of several techniques like

XRD/XRF and imaging to enforce and support the possible hypothesis there-here presented was necessary.

Table 4 compiles the capabilities of the systems employed in this investigation to understand the general trend of geo-environment. It is also summarized the ability of how specific each instrument and its reliability could be to characterize geological samples. Furthermore, the application of the different techniques presented, mainly vibrational methods, and their comparison using twin Martian prototype on analogue samples can provide insights into the strengths and limitations. In our case, the present order to evaluate geo-environments, as well as, to characterize a future selected target should be ordered as follow: Micro-Imaging systems→ Raman Spectroscopy (RLS Instrument) + Infrared Spectroscopy (MicroOmega Instrument)→XRD/XRF (X-ray diffraction and fluorescence – MSL-CheMin) → Mössbauer Spectroscopy (MIMOS-II). Besides, the order was done taking into consideration, in first and last position, the ones already used in space.

The IR spectral mapping from CRISM has found several occurrences of major geochemical alteration of igneous precursors, such as the zeolites. There are more than one candidate mineral to fulfill this analysis due to the closeness in their component elements and their stoichiometry [9,35–37]. Among the most important zeolites, it should be mentioned natrolite, prehnite, phillipsite, chabazite and stilbite, where some of them have been proposed or detected [35,37]. A simple direct comparison of the database presented by B. C. Clark et al (2014) shows that Si/Al ratio of the phillipsite with some Na, K, Ca is 1.85 [37]. However, a more detailed analysis in future research with different samples with the presence of zeolites could be a good complementation for the Raman spectroscopy (as our technique to determine the structure) and the supplementing elemental analysis techniques. Following the

recent discoveries from MSL-Curiosity´s CheMin on Yellow Knife Bay encompass the major elements compared to the Martian soils [38]. Our results show some similarities in the elemental composition being in accordance with the evaluated analysis obtained [37,38]. Their results confirm that alteration products present the trend of elemental composition as follow:

1) For Martian soils: $(CaO+Na_2OK_2O)/ (CaO+Na_2OK_2O+MgO+FeO)$ is mainly between 50 and 80%; $(CaO+Na_2OK_2O)/ (CaO+Na_2OK_2O+Al_2O_3)$ is among 10 to 40%; and $(Al_2O_3)/ (MgO+FeO+Al_2O_3)$ is between 70 and 90%.
2) For Yellowknife Bay: $(CaO+Na_2OK_2O)/ (CaO+Na_2OK_2O+MgO+FeO)$ is mainly between 70 and 80%; $(CaO+Na_2OK_2O)/ (CaO+Na_2OK_2O+Al_2O_3)$ is among 10 to 20%; and $(Al_2O_3)/ (MgO+FeO+Al_2O_3)$ is between 85 and 90%.

Conclusions

The results presented in this work can be concluded considering the following points of view from vibrational spectroscopy passing through: (1) theoretical analysis of zeolites by vibrational spectroscopy, (2) the test of twin instrument, (3) the synergy of combined analysis, (4) comparison with other Martian environment and methods of detection as well, and (5) the complete identification of the mineralization of the Ca-phillipsite (by IR-Raman spectroscopy, mainly) complementing the current hypothesis proposed up to now.

The vibrational analytical tools showed that Raman spectroscopy with the Infrared spectroscopy is capable to detect and analyze hydrothermal minerals and to get the first stage of correlation/evaluation about the possible geology of the mineral of interest. Thus, the results reveal that Raman technique is really powerful when it comes to detect different

possible environment by matching the minerals around the spot. However, it has been observed that theoretical considerations, such as group theory of possible vibrational mode, must be carried out in parallel for a proper mineral identification.

The support on the other instruments like LIBS, XRF and SEM-EDS strongly increased the success and totally complemented the current analysis carried out by vibrational spectroscopy. The overall analysis and general perspective allowed to get a clear identification of the Ca-phillipsite not presented in detail up to now and, also enforcing the hypothesis presented in previous research about the origin of the zeolite in south of Tenerife. Furthermore, new insight and consideration has been done about the special case of the volcano of Las Arenas zeolitization process due to the high Ca-content detected in the samples.

Finally, the results enforce the use and test of twin prototype in selected samples from terrestrial volcanic analogues, like Tenerife, Canary Islands, among others. Nonetheless, the future field-analysis with the portable version would maximize the results. In this regard, the analysis of the second mineralization could be used in Tenerife and considered to have a better understanding of the hydrothermal aqueous alteration on Mars that can produce a range of tell-tale secondary minerals. The methods and the considerations for the zeolites on Mars have been applied like relative proportions (Si/Al) or (Na, K, Ca) as another author proposed. In this regard, a complete compilation of other zeolites totally characterized, as the present research, from other terrestrial outcrop will help to figure out the adequate key-variables for inferring uniqueness of Martian sample, as well as recognition of the signatures of secondary mineralization processes. A more detailed and continuous studies with Raman spectroscopy

on zeolite research will maximize the capabilities of the Raman spectroscopic system on Mars.

Acknowledgement

This work was supported by the MICINN of Spain through the project AYA-2008-04529 for the development of the Raman-LIBS combined spectrometer for the ESA-ExoMars Mission. The first author would like to thank the Ontario Center of Excellence (OCE) for the TalentEdge Funding at York University. The authors would also like to thank Dr. Göstar Klingelhöfer at Mainz University (Mainz, Germany) for the invitation to carry out the measurements with Twin-prototype of the MIMOS-II system.

References

[1] E.A. Lalla, G. López-Reyes, A. Sansano, A. Sanz-Arranz, D. Schmanke, G. Klingelhöfer, et al., Estudio espectroscópico y DRX de afloramientos terrestres volcánicos en la isla de Tenerife como posibles análogos de la geología marciana, Estud. Geológicos. 71 (2015) 1–19. doi:10.3989/egeol.41927.354.

[2] E.A. Lalla, A. Sanz-Arranz, G. Lopez-Reyes, A. Sansano, J. Medina, D. Schmanke, et al., Raman–Mössbauer–XRD studies of selected samples from "Los Azulejos" outcrop: A possible analogue for assessing the alteration processes on Mars, Adv. Sp. Res. 57 (2016) 2385–2395. doi:10.1016/j.asr.2016.03.014.

[3] L. Becerril, I. Galindo, J. Martí, A. Gudmundsson, Three-armed rifts or masked radial pattern of eruptive fissures? The intriguing case of El Hierro volcano (Canary Islands), Tectonophysics. 647–648 (2015) 33–47. doi:10.1016/j.tecto.2015.02.006.

[4] E. Lalla, A. Caramazana Sansano, A. Sanz-Arranz, P. Alonso Alonso, J. Medina García, J. Martinez-frías, et al., Espectroscopía Raman de Basaltos Correspondientes al Volcán de Las Arenas , Tenerife, MACLA - Soc. Española Mineral. 13 (2010) 129–130.

[5] V. Villasante-Marcos, A. Finizola, R. Abella, S. Barde-Cabusson, M.J. Blanco, B. Brenes, et al., Hydrothermal system of Central Tenerife Volcanic Complex, Canary Islands (Spain), inferred from self-potential measurements, J. Volcanol. Geotherm. Res. 272 (2014) 59–77. doi:10.1016/j.jvolgeores.2013.12.007.

[6] J.C. Carracedo, A. Hansen, S. Scaillet, H. Guillou, M. Paterne, U.F. Paleo, La Erupción que Cristobal Colón vio en La Isla de Tenerife (Islas Canarias), Geogaceta. 41 (2007) 39–42.

[7] J.E.G. Hernandez, J.S.N. del Pino, M.M.G. Martin, F.H. Reguera, J.A.R. Losada, Zeolites in pyroclastic deposits in southeastern tenerife (Canary Islands), Clays Clay Miner. 41 (1993) 521–526. doi:10.1346/CCMN.1993.0410501.

[8] H. Ghobarkar, O. Schäf, Y. Massiani, P. Knauth, The Reconstruction of Natural Zeolites: A New Approach to Announce Old Materials by their Synthesis, Kluwer Aca, Springer-Verlag New York Inc., 2003. doi:10.1007/978-1-4419-9142-3.

[9] S.W. Ruff, Spectral evidence for zeolite in the dust on Mars, Icarus. 168 (2004) 131–143. doi:10.1016/j.icarus.2003.11.003.

[10] O. Mousis, J.M. Simon, J.P. Bellat, F. Schmidt, S. Bouley, E. Chassefière, et al., Martian zeolites as a source of atmospheric methane, Icarus. 278 (2016) 1–6.

doi:10.1016/j.icarus.2016.05.035.

[11] A. Basu, J. Schmitt, L. ~J. Crossey, An Argument for Zeolites in Mars Rocks and an Earth Analog, Lunar Planet. Inst. Conf. Abstr. 29 (1998) 1041.

[12] T. Tokano, D.L. Bish, Hydration state and abundance of zeolites on Mars and the water cycle, J. Geophys. Res. Planets. 110 (n.d.). doi:10.1029/2005JE002410.

[13] E.A. Lalla, G. López-Reyes, A. Sansano, A. Sanz-Arranz, J. Martinez-Frías, J. Medina, et al., Raman-IR vibrational and XRD characterization of ancient and modern mineralogy from volcanic eruption in Tenerife Island: Implication for Mars, Geosci. Front. (2015). doi:10.1016/j.gsf.2015.07.009.

[14] B. Downs, S. Robinson, H. Yang, P. Mooney, RRUFF Project, Dep. Geosci. Univ. Arizona. (2015). http://rruff.info/.

[15] J.D. Martin-Ramos, XPowder: A Software Package for Powder X-Ray Diffraction Analysis Powder Methods., (2004).

[16] G. Lopez-Reyes, F. Rull Pérez, A method for the automated Raman spectra acquisition, J. Raman Spectrosc. 48 (2017) 1654–1664. doi:10.1002/jrs.5185.

[17] F. Rull, S. Maurice, I. Hutchinson, A. Moral, C. Perez, C. Diaz, et al., The Raman Laser Spectrometer for the ExoMars Rover Mission to Mars, Astrobiology. 17 (2017) 627–654. doi:10.1089/ast.2016.1567.

[18] N. Buzgar, A.I. Apopei, A. Buzatu, Romanian Database of Raman Spectroscopy, (2009). http://rdrs.uaic.ro.

[19] C. Markovski, J.M. Byrne, E. Lalla, A.D. Lozano-Gorrín, G. Klingelhöfer, F. Rull, et al., Abiotic versus biotic iron mineral transformation studied by a miniaturized backscattering Mössbauer spectrometer (MIMOS II), X-ray diffraction and Raman spectroscopy, Icarus. 296 (2017) 49–58. doi:https://doi.org/10.1016/j.icarus.2017.05.017.

[20] I. Fleischer, G. Klingelhöfer, R. V. Morris, C. Schröder, D. Rodionov, P.A. de Souza, In-situ Mössbauer spectroscopy with MIMOS II, Hyperfine Interact. 207 (2012) 97–105.

[21] F. Pechar, Study of the Raman Polarization Spectra of the Single Crystal Phillipsite, Krist. Und Tech. 16 (1981) 917–920. doi:10.1002/crat.19810160810.

[22] S. V GORYAINOV, M.B. Smirnov, Raman spectra and lattice-dynamical calculations of natrolite, Eur. J. Mineral. 13 (2001) 507–519. http://dx.doi.org/10.1127/0935-1221/2001/0013-0507.

[23] W. Mozgawa, M. Król, K. Barczyk, FT-IR studies of zeolites from different structural groups, Chemik. 65 (2011) 671–674.

[24] N. V. Chukanov, Infrared spectra of mineral species, 1st ed., Springer Netherlands, 2014. doi:10.1007/978-94-007-7128-4.

[25] V.C. Farmer, The Infrared Spectra of Minerals, (1974). https://doi.org/10.1180/mono-4.

[26] G.D. Gatta, P. Cappelletti, A. Langella, Crystal-chemistry of phillipsites from the Neapolitan Yellow Tuff, Eur. J. Mineral. 22 (2010) 779–786. doi:10.1127/0935-

1221/2010/0022-2027.

[27] National Institute of Standards and Technology, LIBS Spectral bands NIST - Database, (2016). http://www.nist.gov/pml/data/asd.cfm.

[28] D.L. Bish, D.F. Blake, D.T. Vaniman, S.J. Chipera, R. V Morris, D.W. Ming, et al., X-ray Diffraction Results from Mars Science Laboratory: Mineralogy of Rocknest at Gale Crater, Sci. . 341 (2013). doi:10.1126/science.1238932.

[29] P. Sarrazin, D. Blake, S. Feldman, S. Chipera, D. Vaniman, D. Bish, Field deployment of a portable X-ray diffraction/X-ray flourescence instrument on Mars analog terrain, Powder Diffr. 20 (2005) 128–133. doi:10.1154/1.1913719.

[30] C. Schröder, Catalogue of Athena Reference (AREF) samples, 2003.

[31] J.G. Stevens, A.M. Khasano, J.W. Miller, H. Pollak, Z. Li, Mössbauer Mineral Handbook, Mössbauer Effect Data Center, Asheville, North Carolina, 2002.

[32] J. Sun, Z. Wu, H. Cheng, Z. Zhang, R.L. Frost, A Raman spectroscopic comparison of calcite and dolomite, Spectrochim. Acta - Part A Mol. Biomol. Spectrosc. 117 (2014) 158–162. doi:10.1016/j.saa.2013.08.014.

[33] N. Rividi, M. van Zuilen, P. Philippot, B. Ménez, G. Godard, E. Poidatz, Calibration of Carbonate Composition Using Micro-Raman Analysis: Application to Planetary Surface Exploration, Astrobiology. 10 (2010) 293–309. doi:10.1089/ast.2009.0388.

[34] Y. Ozpinar, B. Semiz, P.A. Schroeder, Zeolites in mafic pyroclastic rocks from the Sandikli-Afyonkarahisar region, Turkey, Clays Clay Miner. 61 (2013) 177–192. doi:10.1346/CCMN.2013.0610302.

[35] J.C. Bridges, S.P. Schwenzer, R. Leveille, F. Westall, R.C. Wiens, N. Mangold, et al., Diagenesis and clay mineral formation at Gale Crater, Mars, (2014) 1–19. doi:10.1002/2014JE004757.Received.

[36] D. Blake, D. Vaniman, C. Achilles, R. Anderson, D. Bish, T. Bristow, et al., Characterization and calibration of the CheMin mineralogical instrument on Mars Science Laboratory, Space Sci. Rev. 170 (2012) 341–399. doi:10.1007/s11214-012-9905-1.

[37] B.C. Clark, D. Ming, D. Vaniman, R. Wiens, R. Gellert, J.C. Bridges, et al., Eighth International Conference on Mars, in: Eighth Int. Conf. Mars, 2014: pp. 3–4. doi:10.1029/2006JE0.

[38] N. Mangold, O. Forni, G. Dromart, K. Stack, R.C. Wiens, O. Gasnault, et al., Chemical variations in Yellowknife Bay formation sedimentary rocks analyzed by ChemCam on board the Curiosity rover on Mars, J. Geophys. Res. Planets. (2015). doi:10.1002/2014JE004681.Received.

Highlights

- Report of the Raman analysis of the Ca-phillipsite and determination of the Raman mode measured
- Determination of the geological context of mineral on volcanic terrestrial analog by means of Raman spectroscopy and secondary techniques
- Analysis of mineral using the ESA-ExoMars Raman Laser Spectrometer Simulator and other twin system for Martian missions

Combined vibrational, structural, elemental and nuclear analysis of natural phillipsite (zeolite) from historical eruptions in Tenerife, Canary Islands: Implication for Mars

E. A. Lalla[1,2,*], G. Lopez-Reyes[3], A.D. Lozano-Gorrín[4,5] and F. Rull[3]

[1] Centre for research in earth and space science, York University, Petrie Science Building, 4700 Keele St, Toronto, M3J 1P3, Ontario, Canada

[2]Austrian Space Forum, Sillufer 3a, Innsbruck, 6020, Austria

[3]Unidad Asociada UVa-CSIC al Centro de Astrobiología, Parque Tecnológico de Boecillo, Valladolid, Spain.

[4]Departamento de Química, Universidad de La Laguna. Avenida Astrofísico Francisco Sánchez, s/n. 38200 La Laguna, Tenerife, Spain.

[5]Instituto Universitario de Materiales y Nanotecnología. Universidad de La Laguna. Avenida Astrofísico Francisco Sánchez, s/n. 38200 La Laguna, Tenerife, Spain.

Abstract

The outcrop of “Las Arenas Volcano” in Tenerife Canary Island, Spain has been presented as Terrestrial volcanic analog for ancient Mars. It exhibits a great variety of alteration processes and interesting mineralogy such as olivine, pyroxene, feldspar, carbonate, zeolite and different kind of oxide. The analysis has been done by means of measurement techniques used on Mars such as Raman spectroscopy, XRD and Infrared Spectroscopy. A new detailed analysis of the zeolite has been carried out using Raman spectroscopy (standard laboratory technique and space prototype - RLS system), Mossbauer spectroscopy (space twin system – MIMOS-II), XRD (space twin system – TERRA –Insitu ChemMin XRD), Infrared spectroscopy, LIBS and SEM-EDS. The zeolite has been mainly carefully analyzed using vibrational spectroscopy and it has been identified as Ca-phillipsite (Raman and Infrared spectroscopy). The other techniques support and confirmed the results. Moreover, the measurements using the RLS simulator system have been performed and the results show the capabilities RLS Raman system for the ESA Exo-Mars mission. The chemometrical methods for the vibrational mineral detection have been tested showing the advantages of Raman spectroscopy to understand the possible geological context. Also, the proposed diagenesis and formation of the zeolites in southern part of the Tenerife Island have confirmed by space prototypes such as RLS system and MIMOS-II. Furthermore,a new hypothesis about the origin for the special case of Las Arenas Volcano Ca-phillipsite has been proposed

Finally a multi-complementary comparison among the different techniques used on the current studies has been done and, also an analogy with the next space mission has been done. These analyses emphasize the strength of the different techniques and the working synergy of the three different techniques together for planetary space missions. A flow

chart of the analytical procedure has been presented since the micro-imaging to Mossbauer spectroscopy taking in consideration the timing (speed of measurement) for the case of Las Arenas volcano results.

Keywords: Vibrational spectroscopy, Phillipsite, Planetary science, Raman spectroscopy.

Introduction

The volcanic activity of the island of Tenerife has been studied due to the interesting results it brings when it comes to volcanic prediction, geological evolution of Earth, geochemistry, etc. In fact, the historical eruptions are of special interest since the characterization of the natural samples and the mineral species allows scientists to obtain and elucidate accurate results of the past of Mars [1–3]. In the case of the Canary Islands, the main advantage of the historical eruptions is that they have been well documented throughout history. Among the most important historical eruptions that took place in Tenerife, it is important to mention: 1) the triple fissure Fasnia, Siete Fuentes and volcano of Las Arenas (in 1704 and 1705) [4] , 2) the eruption of Montaña Negra in Garachico (in 1706), 3) the volcano of Pico Viejo, Chahorra (in 1798) [5] and the volcano Chinyero (in 1909) [6].

The volcanoes of Fasnia, Siete Fuentes, Las Arenas and Chinyero are located in the southeastern part of the island where the occurrence of zeolites in the pyroclastic and basaltic deposits has been documented [7]. Furthermore, the geologic conditions are very favorable for some specific zeolite formations. Among the most important reported minerals are phillipsite, chabazite and analcime, being the phillipsite the most abundant from the previous studies. Also, Garcia-Hernandez et al. (1993) concluded that the zeolites were formed by the action of water vapor trapped within the pores of the

volcanic glasses [7]. In this sense, the high temperature and closed system conditions create favorable rapid method to nucleate and grow zeolite from water vapor and volcanic glass [8].

Special consideration should be taken into account about the zeolites in the Martian environments; it has been suggested that these minerals could have strong impact in the Martian environment and atmosphere [9]. There exists the possibility that zeolites could be a reservoir system of the methane in the Martian subsurface [10]. Furthermore, another recent hypothesis suggests that the zeolite distribution could be present in certain dust-poor regions affecting the diurnal atmospheric water cycle along the seasons [11,12].

On this research, a complete analysis of zeolite detected in certain samples from the volcano of Las Arenas using a complete combination of present and future space instrumentation for planetary science focused on Mars is presented. The volcanic outcrop has been already proposed as possible terrestrial analog for the ExoMars Mission and it has been fully analyzed by means of Raman spectroscopy to complement the science behind the Raman Laser Spectrometer (RLS). However, a detailed analysis of certain secondary mineralization detected on these samples has not been done yet using techniques already or about to be applied in Martian Rover missions. The detailed analysis has been carried out by Raman spectroscopy, Laser induced breakdown spectroscopy and X-ray diffraction (XRD) working in synergy using certain twin prototype instruments such RLS-simulator and Terra-Insitu XRD. In addition, SEM-EDX microscopy and Infrared spectroscopy have helped to strongly complement the results and characterize the zeolite detected.

Experimental results and sampling methods

The sample set was collected by picking out samples on the studied areas on expeditions to the Canary Islands in 2010, being all of them catalogued and photographed. The detailed pictures of the samples have been documented and the detailed mineralization is presented on E. Lalla et al. (2015) [13]. The main minerals detected on the outcrop are summarized on Table 1. The SEM-EDS measurements were obtained by using a Scanning Electron Microscope FEI - Quanta 200FEG. The system is equipped with electron cannon emission type with Schottky filaments using an acceleration voltage of 30 kV with EDS Oxford Inca Energy 350, equipped with secondary electron detectors. For this analysis, no sample preparation was necessary and the measurements were directly performed on the bulk samples. The images of the different vesicles studied were obtained by Nikkon SMZ 800 microscope system.

The XRD patterns were obtained with a Terra XRD-diffractometer instrument based on the MSLCheMin concept with a 1024x256 detector working in 2D-CCD mode. The XRD source is cobalt X-ray tube of 30 Kv-300 uA. The preparation consisted on the powdering of a minimum part of the samples (2−4 mg) and sieved with a granulometry lower than 150 mm. The analysis and identification was done using the software from Terra-In-Situ XPowder by pattern matching with the JCPDS database and manually double checked with the XRD diffractogram from RRUFF and using Crystal Sleuth [14,15].

The micro-Raman measurement of the samples was performed with a microscope Nikon Eclipse E600 coupled to a spectrometer KOSI Holospec f/1.8i, with best spectral resolution of 5 cm^{-1}, illuminated by a laser REO LSRP-3501 He-Ne (632.8 nm wavelength). The detection was performed by a CCD Andor DV420A-OE-130. The laser power used on the sample was 14 mW with a minimum spot diameter of 15 μm. The Raman mapping of the bulk surface of the sample was done with a Micro-Raman

Prior Proscan II motorized stage in automatic mode in order to detect the different compositional mineralization. The RLS Raman automatic measurement were done by the ExoMars RLS Simulator in automatic mode (acquiring several spectra per sample, with automatically calculated integration time and number of accumulations at each point [16]. The laser wavelength corresponds to 532 nm with a spot size: 50 microns and with irradiances of 0.25 and 1 kW/cm^2 [16,17] .

The FT-Raman analysis was performed with a Fourier Transform Raman (FT-Raman) Bruker RSF 100/S, which allows the analysis of high fluorescence samples, making it more suitable for some samples than the visible Raman equipment. The FT-Raman spectrometer is composed by a Nd:YAG Laser at 1064 nm, spectrograph with spectral range 851−1695 nm (NIR) and best spectral resolution of 2 cm^{-1}. The detector is a Bruker CCD model D418T cooled by liquid N2. The working conditions achieved a spectral resolution of 4 cm^{-1} and a diameter spot of 100 mm approximately.

Fort the LIBS measurements, the system used was a StellarNet PORTA-LIBS 2000 with a spectral range from 400 to 850. The excitation source was 1064 nm Nd:YaG laser with a pulse duration of 6 ns and a total energy of 1 GW cm^{-2} onto the spot.

The results were directly obtained from the part sample material without any sample preparation. The spectroscopic analysis was done processed by means of gaussian curve fitting in order to determine the correct band position, intensity, FWHM and spectral profile for the different mineral phases detected. We used Bruker OPUS to calculate the fitting on the sample and following the standard procedure available on the software such as spectra smoothing (if it is required), background subtraction, normalization and Levenberg-Marquardt curve fitting. The mineral identification has been done according

the RRUFF database, Romanian Raman Database and other references that will be included in the discussion section [14,18].

The Mössbauer spectra were collected with a copy of the MIMOS II spectrometer from the past NASA-MER-mission (AK Klingelhoefer, Mars Mössbauer Group, Mainz, Germany). The system has a Co^{57}/Rh source with an intensity of about 50 mCi. The measurements have been performed at room temperature and without sample preparation in a backscattering geometry. The method of analysis was the same as C. Markowski et al., (2017) and E. Lalla et al., (2016) [2,19,20]

Analytical results

Figure 1 shows an example of the vesicles where the zeolites have been detected from previous studies.

Raman Spectroscopy Analysis

The phillipsite minerals with the chemical formula $(Ca,Na_2,K_2)_3Al_6Si_{10}O_{32}{\cdot}12H_2O$ crystalize in a monoclinic system with the space group $P\ 2_1/m$ [21]. Indeed, it has been reported that the crystal lattice of this zeolite is mainly formed by interconnected long chains of (Al, Si)O_4 tetrahedra. Every single chain is a subsequently combination of four tetrahedral and the water molecules and/or cations are localized in the channels formed between the principal and secondary chains [21]. The theoretical factor group analysis already calculated has [21]:

$$T_{Opt} = 147A_1^z(IR,R) + 146A_2(R) + 146B_1^X(IR,R) + 146B_2^Y(IR,R) \quad (1)$$

Where the symmetric modes $A_1(z)$, $B_1(x)$ and $B_2(y)$ are active in the spectra for both Raman and Infrared modes. In this sense, the Raman spectrum is a combination of the longitudinal ad transverse vibrational modes (LO and TO) [21]. Also, it has to be

considered that is not possible to separate the LO and TO modes due to the fact that these modes could be degenerated. However, F. Pechar et al (1981) presented the experimental vibrational results and it all can be divided in the main factor groups [21]: 1) the optical modes of the crystal lattice (from 50 to 600 cm^{-1}); 2) the internal vibrations of the water molecules (from 1600 to 3700 cm^{-1}); 3) the internal vibrations of the bonds from the Al/Si-O_4 (from 400 to 1000 cm^{-1}) ; and 4) the external vibrations of H_2O molecules (from 300 to 680 cm^{-1}). Table 2 compiles Gaussian fitting position from some spectra obtained from the Micro-Raman analysis with the complementary theoretical assignment from F. Pechar et al (1981) and other phillipsite from RRUFF like Ca-phillipsite (R050078), K-phillipsite (R140774) and Na-phillipsite (R061094) [14,21]. Figure 2 shows the different spectra from Table 2 and the graphical band assignment. A similar analysis was carried out using the spectra obtained by the ESA-ExoMars RLS simulator. The samples were automatically aligned and best exposure and acquisition were automatically calculated from the RLS software. The band positions from Gaussian fitting of the Raman bands are listed in Table 3 and Figure 3 shows the spectra from the same spot analyzed in Figure 1.

Infrared Spectroscopy Analysis

Following the Eq. (1), the IR spectrum of the phillipsite presents the following IR active modes and they can be assigned as: 1) asymmetric stretching vibration of the bridge bonds ν_{asym}(Si-O-Si) and ν_{asym}(Si-O,Al) at ~1000 cm^{-1}; 2) the symmetric stretching vibrations of the bridge bonds ν_{sym}(Si-O-Si) at ~720 cm^{-1}, 3) the symmetric stretching vibrations of the bridge bonds ν_{sym}(Si-O-Al) at ~670 cm^{-1}, 3) the complex band from the combined symmetric stretching vibrations ν_{symm} (Si-O-Si) and bending vibrations – δ(O-Si-O) at ~550 cm^{-1}, 4) the bending vibrations δ(O-Si-O), occurring in 468 cm^{-1} and 5) the bending vibrations δ (O-Si-O)/δ(O-Al-O) around 377 cm^{-1} [21,22]. Besides, the

zeolite uses to present the external vibrations of H_2O molecules. Among the most intense, it can be observed the H_2O at ~3300 cm^{-1}, asymmetric vibrations of (O-H) at 3600 cm^{-1} and the (Al,Si)-OH vibrations around 1650 cm^{-1}. Table 3 summarizes all the principal assigned Infrared bands detected on the Las Arenas Volcano´s phillipsite and a comparison with the IR spectra available at RRUFF has been done (standard selected: Na-phillipsite (R061094), K-phillipsite (R140774), Ca-phillipsite (R050078)) [14,22]. Figure 4 compiles the Gaussian fitting analysis from Table 3 containing the IR spectrum of phillipsite, the other points present similar behavior. On the other hand, the comparison with a Na-phillipsite (Sif Z99) from N. V. Chukanov (2014) shows a similar behavior [23]. It has been observed that main intense band (ν_{asym}(Si-O-Si) and ν_{asym}(Si-O,Al)) is lightly shifted to higher values around 1000 cm^{-1}, however the band position of ν_{sym}(Si-O-Al) is more or less in a pretty similar position. The bands related to ν(Al,Si)-OH at ~1630 cm^{-1} and ν_{assym}(O-H) / H_2O present quite similar positions in both spectra (Na-phillipsite and Las Arenas Negras Volcano Phillipsite) [22–24]

Scanning Electron Microscopy

The Scanning Electron Microscopy analysis in Figure 5 shows the existence of the phillipsite that can be confirmed by pseudo-orthorhombic structure with an elongation along b axis. The points (c) and point (d) present similar structures as the points (a) and (b). Thus, no significant difference in shape and size was observed among the different samples of different outcrops. The formation of the phillipsite inside de vesicles of the bulk matrix is accordance with other similar results occurring in radiating clusters [7,25]. On the other hand, the SEM also shows the occurrence of other crystal formation such as the calcite. Taking into consideration the crystal Atlas, it can be observed the calcite by observing the different trigonal structures with a point group 32/m. Calcite shows to be coarse grained and possibly cement-filling central parts of vesicles and the

inter-granular spaces. The chemical analyses of the phillipsite from the different sample point are reported in Table 5.

Laser Induced Breakdown Spectroscopy (LIBS)

LIBS data were acquired in the visible range (from blue & violet, visible and near infrared wavelengths) on the point (d) (see Figure 1) and it is summarized in Figure 6. The identification of the peaks were done using the NIST LIBS library and Figure 6 only illustrates the most of the major elements detectable over these wavelength ranges [26]. The elements identified in the LIBS spectra are Fe, Si, Al, Ca, K, O, Mg, C and Na. The elements detected match with the elemental composition of the general stoichiometry of the phillipsite in combination with the calcite. Furthermore, a small variability concerning the peak intensities has been found, being an indicator of changes in the elemental abundance. The most notable variability corresponds to the ones assigned to C, O and Ca, which could be related to the abundance of calcite in the different vesicles and/or laser spot used for measurements. The elements detected match and they can be confirmed by the SEM-EDS results in Table 5. However, some elements, like Ti and P, were not detected due to resolution of the spectrometer and laser power (to create plasma on Ti/P).

X-Ray Diffraction/X-Ray fluorescence

The mineralogy obtained by the XRD in one of the samples shows the detection of the phillipsite and calcite in the diffraction pattern. Figure 7 presents the mineral identification with the standard RRUFF samples (Ca-phillipsite (R050078), K-phillipsite (R140774) and Na-phillipsite (R061094) for a better appreciation of the phillipsite detection [14]. However, there is also other minerals quartz, feldspar, clays (detected and not patterned), olivine and pyroxenes due to the extraction. The extraction

method was done by carefully scratching the minerals (phillipsite and calcite) from one of the vesicle. Thus, the vesicle minerals also contain the bulk main mineralization from samples which can be confirmed from Table 1 and from previous results in E. Lalla et al (2015) [13]. On the other hand, the confirmation of the existence of the Ca-phillipsite has been checked by two other methods: 1) comparison with the XRD diffraction pattern from standard RRUFF samples (a) Na-phillipsite (R061094), (b) K-phillipsite (R140774), (c) Ca-phillipsite (R050078) [14] and also 2) by comparing the XRD results presented on J. E. Garcia Hernandez [7].

The Terra Insitu XRD is capable to obtain also X-ray fluorescence measurements. The results obtained are shown in Figure 8, where the elements detected by internal analysis of the instrument shows the detection of Ca, Si, Al, Ti, Fe, and K that correspond to the elements that form part of the minerals and they match with LIBS elemental identification and SEM-EDX elemental identification-quantification. However, there are some limitations on the XRF system from the Terra Insitu to be considered due to the fact that the XRF mode system was designed as a support method to complement the XRD [27,28]. Thus, XRF is a semi-quantitative elemental analytical system to enforce the XRD mode. First of all, there is a reduced sensitivity below Si transitions due to Be window and chip technology used on the system. Also, the Co from the source used caused high intense diffracted peaks masking others. Finally there also exists an over estimation of Fe, Mn and Cr due to the contamination from the CCD housing and stainless steel of the structure [28].

Mossbauer Analysis

Mössbauer spectroscopy analysis has been performed measuring some selected samples where the phillipsite was visually observed from E. Lalla et al (2015) and E. Lalla et al

(2010) [4,13]. The hyperfine parameter (as isomer shift (IS), quadrupole splitting (QS) and spectral line width) and the corresponding minerals detected, derived from the data, are listed in Table 6 and shown in Figure 9. The different sub-spectral areas obtained by a band fitting from the different samples show Fe-content minerals only following the methods in the references [2,19,20] and the standard used for comparison were from [29,30]. The results showing the presence of olivine, pyroxene, magnetite, goethite, and oxide phase with different degrees of crystallinity have been also confirmed on E. Lalla et al (2015) [4,13].

Discussion

The vibrational analysis from the theoretical perspective using the group theory has been confirmed using the experimental results and carefully analyzed with a Gaussian profile fitting. During the analysis, it has been compared with several standards Raman from RRUFF using the 3 different phillipsitic kind such Ca, Na and K- phillipsite. By taking into consideration the Raman band profiling, the phillipsite corresponds to a Ca-phillipsite by the match of the ν_{symm}(O-(Al,Si)-O) at 419, ν_{int} (Al,SiO_4) at 480 and ν_{int} (Al,SiO_4) at 505 cm^{-1}. The subsequent confirmation was carried out by the RLS simulator of same Raman vibrations and detection of other bands like ν_{symm}(Al,Si)-O at ~760 cm^{-1}. Furthermore, the RLS system has shown more sensitivity and water and OH^- related vibrations bands at ~120-140 cm^{-1}, at ~1630 and ~3500-3600cm^{-1} have been also detected (See Tables 2 and 3). On the other hand, the ν_{assym}(Al,Si)-O Raman bands, located between 1000 and 1150 cm^{-1}, were observed on the Raman spectra from the RRUFF standards. However, the same bands in our samples were not detected due to the fact of having low intensity peak value and they were masked by the intense band of the calcite.

The technique based on vibrational spectroscopy like the Infrared spectroscopy also matched with Ca-phillipsite mineral type. The main confirmation has been done by the ν_{sym}(Si-O-Al) at ~670, ν_{sym}(Si-O-Si) at ~730 and the ν_{asym}(Si-O-Si)/ν_{asym}(Si-O,Al) at ~989 cm^{-1}. Also, the water vibration predicted by Pechar et al. (1981) [21] was measured being at ~1638 (ν(Al,Si)-OH), ~3200 ($\nu(H_2O)$ and ~3400-3600 (ν_{assym} (O-H)) cm^{-1}. The calcite was detected on the spectra and it is presented in Figure 4. Furthermore, the Infrared spectroscopy shows that most intense bands were not overlapping the other bands from Las Arenas volcano Ca-phillipsite.

The elemental composition analysis carried out by the portable instrumentation like LIBS and XRF were in agreement by the detection of iron (Fe), potassium (K), sodium (Na), magnesium (Mg), aluminum (Al), silicon (Si), carbon (C), oxygen (O) and calcium (Ca). Concerning both techniques, LIBS shows more sensitivity to the elements given the limitation of the XRF mode of the Terra-Insitu aforementioned. However, in both analyses, Ca has been commonly detected as the major compared to Na or K by comparing the intensity, helping to confirm calcic nature of the mineral from the vibrational analysis (Raman-IR). Also, it has been detected the C element on both techniques, which could correspond to the calcite detected on the samples. The SEM-EDS confirmed and determined the elemental compositions of the different vesicles measured by LIBS and XRF. In the different points (a), (b) and (d), the results show a similar behavior with the exception of the vesicle (c) where it can have a bigger concentration of calcite given the high values of CO. Taking into account the Si/Al ratio, it has been observed that phillipsite from Las Arenas volcano presents the following values: (a) 2.18, (b) 2.20, (c) 2.12, and (d) 1.95. The current values match with the results from previous studies, where the general trend is from 2.00 to 2.15 approximately [7]. In the special case of the Las Arenas volcano, phillipsite, compared

to the other zeolites detected in the south of Tenerife, presents higher values of Ca concentration.

The XRD results showed the presence of the phillipsite in the presence of the bulk matrix rock forming minerals like feldspars, pyroxenes, olivines and quartz. In Figure 7, the analysis of the extracted powdered from one vesicle and compared with the RRUFF XRD standards is shown. It can be observed that the presence of the principal peaks may be masked with other more active minerals for XRD given the crystallinity and crystal orientation during the measurement. The principal values presented in J. E. Garcia Hernandez et al (1993) [7] match with the results obtained in the present research. Also, J. E. Garcia Hernandez et al (1993) has discussed that Tenerife´s phillipsites are quite different from the other phillipsite (such as Italian phillipsites presented on [7]) on the due to the fact that mineral presents lower values for the c-axis and, therefore, smaller unit-cell volumes [7].

Finally, the Mossbauer analysis carried out at Mainz University showed the detection of the principal rock forming minerals from the matrix. Among the principals minerals detected, one can find olivine, pyroxene, amorphous phases of Fe_2O_3 and magnetite.

In previous results, J. E. Garcia-Hernandez et al (1993) presented Tenerife phillipsites as an intermediate between the diagenetic and the deep-sea ones [7]. Phillipsites from deep-sea sediments and saline lake deposits have larger Si/Al ratios, which is not the case of Las Arenas volcano. The sequence of occurrence and paragenesis found out is the following: Glass → Phillipsite → Phillipsite + Analcime → Phillipsite + Analcime + Feldspar [7,13]. Furthermore, the hypothesis about origin of zeolite kind could be confirmed by the Raman-IR spectroscopy, where the water vapor trapped interact with the glass particles by hydrothermalism promoting the formation of zeolites [7]. Thus,

the water vapor in contact with the melting volcanic glass in closed-system conditions promotes the glass hydration, with a subsequent dissolution and nucleation. Finally, when the temperature starts to decrease, the growth of zeolite crystals can be originated [7,25]. Nonetheless, in the special case of Las Arenas volcano and according with the current measurements, the phillipsite is a Ca-enriched solid solution. The origin could probably happen by a direct formation in Ca-bearing solutions or by post-zeolitization cation exchange among the Ca, Na and K. Finally the formation of the accessory calcite could be related to CO_2 gases in combination with H_2O providing hydrolysis reactions [31]. The carbonate ions (CO_3^{2-}) could be combined with excess of Ca and started to form calcite. The detection of calcite by Raman-IR spectroscopy and XRD/XRF and LIBS confirms the enrichment of Ca in the phillipsite and calcite suggesting a really low CO_2 fugacity during the zeolitization process. However, more detailed studies to support this idea from the data presented in this research will be needed and it must be regarded as a hypothesis.

The vibrational spectroscopic analysis, like Raman and Infrared, is a powerful tool giving new perspectives and viewpoint of the ideas as well as complement about the paleogenesis of the Ca-phillipsite of Las Arenas. However, a conjunction of several techniques like XRD/XRF and imaging to enforce and support the possible hypothesis there-here presented was necessary.

Table 6 compiles the capabilities of the systems employed on this investigation to understand the general trend of geo-environment. It is also summarized the ability of how specific could be each instrument and its reliability to characterize geological samples. Furthermore, the application of the different technique presented, mainly vibrational methods, and their comparison using twin Martian prototype on analogue samples can provide insights into the strengths and limitations. In our case, the present

order to evaluate geo-environments, as well as to characterize the selected target should be ordered as follow: Micro-Imaging systems→ Raman Spectroscopy (RLS Instrument) + Infrared Spectroscopy (MicroOmega Instrument)→XRD/XRF (X-ray diffraction and fluorescence – MSL-CheMin) → Mossbauer Spectroscopy (MIMOS-II). Figure 10 compiles a flowchart following the optimized analysis considering the timing of measurements and analysis. Besides, the order was done taking into consideration, in first and last position, the ones already used in space (by the known possible timing) (see Table 8).

The IR spectral mapping from CRISM has found several occurrences of major geochemical alteration of igneous precursors, such as the zeolites. There are more than one candidate mineral to fulfill this analysis due to the closeness in their component elements and their stoichiometry [9,32–34]. Among the most important zeolite, it should be mentioned natrolite, prehnite, phillipsite, chabazite and stilbite where some of them have been proposed or detected [32,34]. A simple direct comparison of the database presented by B. C. Clark et al (2014) shows that Si/Al ratio of the phillipsite with some Na, K, Ca is 1.85 [34]. However a more detailed analysis in future research with different samples with the presence of zeolites could be a good complementation for the Raman spectroscopy (as my technique to determine the structure) and the supplementing elemental analysis techniques. Following the recent discoveries from MSL-Curiosity´sCheMin on Yellow Knife Bay encompass the major elements compared to the Martian soils [35]. Our results show some similarities in the elemental composition being in accordance with the evaluated analysis obtained [34,35]. Their results confirm that alteration products present the trend of elemental composition as follow:

1) For Martian soils: ($CaO+Na_2OK_2O$)/ ($CaO+Na_2OK_2O+MgO+FeO$) is mainly between 50 and 80% ; ($CaO+Na_2OK_2O$)/ ($CaO+Na_2OK_2O+Al_2O_3$) is among 10 to 40%; and (Al_2O_3)/ ($MgO+FeO+Al_2O_3$) is between 70 and 90%.
2) For Yellowknife Bay: ($CaO+Na_2OK_2O$)/ ($CaO+Na_2OK_2O+MgO+FeO$) is mainly between 70 and 80%; ($CaO+Na_2OK_2O$)/ ($CaO+Na_2OK_2O+Al_2O_3$) is among 10 to 20%; and (Al_2O_3)/ ($MgO+FeO+Al_2O_3$) is between 85 and 90%.

Conclusions

The results presented in these work can be concluded considering the following points of view from vibrational spectroscopy passing through: 1) theoretical analysis of zeolites by vibrational spectroscopy, 2) the test of twin instrument, 3) the synergy of combined analysis, 4) comparison with other Martian environment and methods of detection as well, and 5) the complete identification of the mineralization of the Ca-phillipsite (by IR-Raman spectroscopy, mainly) complementing the current hypothesis proposed up to now.

The vibrational analytical tools showed that Raman spectroscopy with the Infrared spectroscopy is capable to detect and analyze hydrothermal minerals and to get the first stage of correlation/evaluation about the possible geology of the mineral of interest. Thus, the results reveal that Raman technique is really powerful when it comes to detect different possible environment by matching the minerals around the spot. However, it has been observed that theoretical considerations, such as group theory of possible vibrational mode, must be carried out in parallel for a proper mineral identification.

The support on the other instruments like LIBS, XRF and SEM-EDS strongly increased the success and totally complemented the current analysis carried out by vibrational spectroscopy. The overall analysis and general perspective allowed to get a clear

identification of the Ca-phillipsite not presented in detail up to now and, also enforcing the hypothesis presented in previous research about the origin of the zeolite in south of Tenerife. Furthermore, new insight and consideration has been done about the special case of the Volcano of Las Arenas zeolitization process due to the high Ca-content detected on the samples.

Finally, the results enforce the use and test of twin prototype in selected samples from terrestrial volcanic analogues, like Tenerife, Canary Islands, among others. Nonetheless, the future field-analysis with the portable version would maximize the results. In this regards, the analysis of the second mineralization could be used in Tenerife and considered to have a better understanding of the hydrothermal aqueous alteration on Mars that can produce a range of tell-tale secondary minerals. The methods and the considerations for the zeolites in Mars have been applied like relative proportions (Si/Al) or (Na, K, Ca) as other author proposed. In this regard, a complete compilation of other zeolites totally characterized, as the present research, from other terrestrial outcrop will help to figure out the adequate key-variables for inferring uniqueness of Martian sample, as well as recognition of the signatures of secondary mineralization processes. A more detailed and continuous studies with Raman spectroscopy on zeolite research will maximize the capabilities of the Raman spectroscopic system on Mars.

Acknowledgement

The work was supported by the MICINN of Spain through the project AYA-2008-04529 for the development of the Raman-LIBS combined spectrometer for the ESA-ExoMars Mission. The first author would like to thanks to the Ontario Cluster of Excellence (OCE) for the TalentEdge Funding at York University-MDA. The authors would also like to thank Dr. Göstar Klingelhöfer at Mainz University (Mainz, Germany)

for the invitation to carry out the measurements with Twin-prototype of the MIMOS-II system.

References

[1] E.A. Lalla, G. López-Reyes, A. Sansano, A. Sanz-Arranz, D. Schmanke, G. Klingelhöfer, et al., Estudio espectroscópico y DRX de afloramientos terrestres volcánicos en la isla de Tenerife como posibles análogos de la geología marciana, Estud. Geológicos. 71 (2015) 1–19. doi:10.3989/egeol.41927.354.

[2] E.A. Lalla, A. Sanz-Arranz, G. Lopez-Reyes, A. Sansano, J. Medina, D. Schmanke, et al., Raman–Mössbauer–XRD studies of selected samples from "Los Azulejos" outcrop: A possible analogue for assessing the alteration processes on Mars, Adv. Sp. Res. 57 (2016) 2385–2395. doi:10.1016/j.asr.2016.03.014.

[3] L. Becerril, I. Galindo, J. Martí, A. Gudmundsson, Three-armed rifts or masked radial pattern of eruptive fissures? The intriguing case of El Hierro volcano (Canary Islands), Tectonophysics. 647–648 (2015) 33–47. doi:10.1016/j.tecto.2015.02.006.

[4] E. Lalla, A. Caramazana Sansano, A. Sanz-Arranz, P. Alonso Alonso, J. Medina García, J. Martinez-frías, et al., Espectroscopía Raman de Basaltos Correspondientes al Volcán de Las Arenas , Tenerife, MACLA - Soc. Española Mineral. 13 (2010) 129–130.

[5] V. Villasante-Marcos, A. Finizola, R. Abella, S. Barde-Cabusson, M.J. Blanco, B. Brenes, et al., Hydrothermal system of Central Tenerife Volcanic Complex, Canary Islands (Spain), inferred from self-potential measurements, J. Volcanol.

Geotherm. Res. 272 (2014) 59–77. doi:10.1016/j.jvolgeores.2013.12.007.

[6] J.C. Carracedo, A. Hansen, S. Scaillet, H. Guillou, M. Paterne, U.F. Paleo, La Erupción que Cristobal Colón vio en La Isla de Tenerife (Islas Canarias), Geogaceta. 41 (2007) 39–42.

[7] J.E.G. Hernandez, J.S.N. del Pino, M.M.G. Martin, F.H. Reguera, J.A.R. Losada, Zeolites in pyroclastic deposits in southeastern tenerife (Canary Islands), Clays Clay Miner. 41 (1993) 521–526. doi:10.1346/CCMN.1993.0410501.

[8] H. Ghobarkar, O. Schäf, Y. Massiani, P. Knauth, The Reconstruction of Natural Zeolites: A New Approach to Announce Old Materials by their Synthesis, Kluwer Aca, Springer-Verlag New York Inc., 2003. doi:10.1007/978-1-4419-9142-3.

[9] S.W. Ruff, Spectral evidence for zeolite in the dust on Mars, Icarus. 168 (2004) 131–143. doi:10.1016/j.icarus.2003.11.003.

[10] O. Mousis, J.M. Simon, J.P. Bellat, F. Schmidt, S. Bouley, E. Chassefière, et al., Martian zeolites as a source of atmospheric methane, Icarus. 278 (2016) 1–6. doi:10.1016/j.icarus.2016.05.035.

[11] A. Basu, J. Schmitt, L. ~J. Crossey, An Argument for Zeolites in Mars Rocks and an Earth Analog, Lunar Planet. Inst. Conf. Abstr. 29 (1998) 1041.

[12] T. Tokano, D.L. Bish, Hydration state and abundance of zeolites on Mars and the water cycle, J. Geophys. Res. Planets. 110 (n.d.). doi:10.1029/2005JE002410.

[13] E.A. Lalla, G. López-Reyes, A. Sansano, A. Sanz-Arranz, J. Martinez-Frías, J. Medina, et al., Raman-IR vibrational and XRD characterization of ancient and

modern mineralogy from volcanic eruption in Tenerife Island: Implication for Mars, Geosci. Front. (2015). doi:10.1016/j.gsf.2015.07.009.

[14] B. Downs, S. Robinson, H. Yang, P. Mooney, RRUFF Project, Dep. Geosci. Univ. Arizona. (2015). http://rruff.info/.

[15] J.D. Martin-Ramos, XPowder: A Software Package for Powder X-Ray Diffraction Analysis Powder Methods., (2004).

[16] G. Lopez-Reyes, F. Rull Pérez, A method for the automated Raman spectra acquisition, J. Raman Spectrosc. 48 (2017) 1654–1664. doi:10.1002/jrs.5185.

[17] F. Rull, S. Maurice, I. Hutchinson, A. Moral, C. Perez, C. Diaz, et al., The Raman Laser Spectrometer for the ExoMars Rover Mission to Mars, Astrobiology. 17 (2017) 627–654. doi:10.1089/ast.2016.1567.

[18] N. BUZGAR, A. APOPEI, Andrei Ionut BUZATU, Romanian Database of Raman Spectroscopy, (2009). http://rdrs.uaic.ro.

[19] C. Markovski, J.M. Byrne, E. Lalla, A.D. Lozano-Gorrín, G. Klingelhöfer, F. Rull, et al., Abiotic versus biotic iron mineral transformation studied by a miniaturized backscattering Mössbauer spectrometer (MIMOS II), X-ray diffraction and Raman spectroscopy, Icarus. 296 (2017) 49–58. doi:https://doi.org/10.1016/j.icarus.2017.05.017.

[20] I. Fleischer, G. Klingelhöfer, R. V. Morris, C. Schröder, D. Rodionov, P.A. de Souza, In-situ Mössbauer spectroscopy with MIMOS II, Hyperfine Interact. 207 (2012) 97–105.

[21] F. Pechar, Study of the Raman Polarization Spectra of the Single Crystal

Phillipsite, Krist. Und Tech. 16 (1981) 917–920. doi:10.1002/crat.19810160810.

[22] W. Mozgawa, M. Król, K. Barczyk, FT-IR studies of zeolites from different structural groups, Chemik. 65 (2011) 671–674.

[23] N. V. Chukanov, Infrared spectra of mineral species, 1st ed., Springer Netherlands, 2014. doi:10.1007/978-94-007-7128-4.

[24] V.C. Farmer, The Infrared Spectra of Minerals, (1974). https://doi.org/10.1180/mono-4.

[25] G.D. Gatta, P. Cappelletti, A. Langella, Crystal-chemistry of phillipsites from the Neapolitan Yellow Tuff, Eur. J. Mineral. 22 (2010) 779–786. doi:10.1127/0935-1221/2010/0022-2027.

[26] National Institute of Standards and Technology, LIBS Spectral bands NIST - Database, (2016). http://www.nist.gov/pml/data/asd.cfm.

[27] D.L. Bish, D.F. Blake, D.T. Vaniman, S.J. Chipera, R. V Morris, D.W. Ming, et al., X-ray Diffraction Results from Mars Science Laboratory: Mineralogy of Rocknest at Gale Crater, Sci. . 341 (2013). doi:10.1126/science.1238932.

[28] P. Sarrazin, D. Blake, S. Feldman, S. Chipera, D. Vaniman, D. Bish, Field deployment of a portable X-ray diffraction/X-ray flourescence instrument on Mars analog terrain, Powder Diffr. 20 (2005) 128–133. doi:10.1154/1.1913719.

[29] C. Schröder, Catalogue of Athena Reference (AREF) samples, 2003.

[30] J.G. Stevens, A.M. Khasano, J.W. Miller, H. Pollak, Z. Li, Mössbauer Mineral Handbook, Mössbauer Effect Data Center, Asheville, North Carolina, 2002.

[31] Y. Ozpinar, B. Semiz, P.A. Schroeder, Zeolites in mafic pyroclastic rocks from

the Sandikli-Afyonkarahisar region, Turkey, Clays Clay Miner. 61 (2013) 177–192. doi:10.1346/CCMN.2013.0610302.

[32] J.C. Bridges, S.P. Schwenzer, R. Leveille, F. Westall, R.C. Wiens, N. Mangold, et al., Diagenesis and clay mineral formation at Gale Crater, Mars, (2014) 1–19. doi:10.1002/2014JE004757.Received.

[33] D. Blake, D. Vaniman, C. Achilles, R. Anderson, D. Bish, T. Bristow, et al., Characterization and calibration of the CheMin mineralogical instrument on Mars Science Laboratory, Space Sci. Rev. 170 (2012) 341–399. doi:10.1007/s11214-012-9905-1.

[34] B.C. Clark, D. Ming, D. Vaniman, R. Wiens, R. Gellert, J.C. Bridges, et al., Eighth International Conference on Mars, in: Eighth Int. Conf. Mars, 2014: pp. 3–4. doi:10.1029/2006JE0.

[35] N. Mangold, O. Forni, G. Dromart, K. Stack, R.C. Wiens, O. Gasnault, et al., Chemical variations in Yellowknife Bay formation sedimentary rocks analyzed by ChemCam on board the Curiosity rover on Mars, J. Geophys. Res. Planets. (2015). doi:10.1002/2014JE004681.Received.

List of Figures

Figure 7. XRD of the powder extracted from a vesicle with a comparison from RRUFF standards. (a) Na-phillipsite (R061094 – in blue), (b) K-phillipsite (R140774 – in blue), (c) Ca-phillipsite (R050078 – in blue) and (d) extracted powdered phillipsite from a vesicle in the Point (d). Minerals: Clays (M-Cl), phillipsite (Php), quartz (Qtz), pyroxene (Py), feldspar (Fsp), olivine (Ol), and calcite (Cal).

Figure 8. X-ray Fluorescence of the powder extracted from a vesicle with the corresponding elemental assignation.

Figure 9. Representative Mössbauer spectra from Las Arenas volcano outcrop observed on the fitting process of the experimental data presenting the principal and secondary mineral phases.

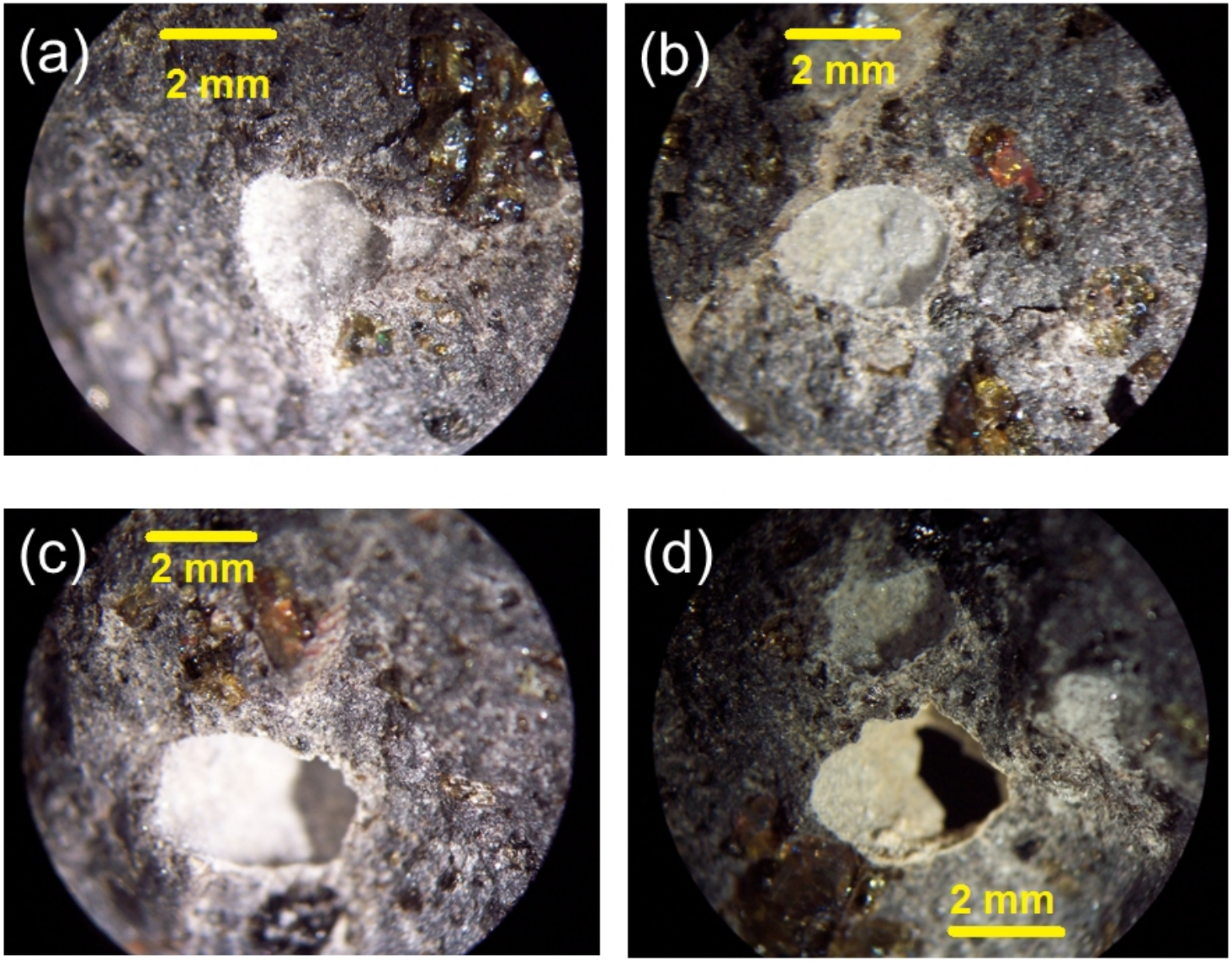
(a)
2 mm
(b)
2 mm
(c)
2 mm
(d)
2 mm

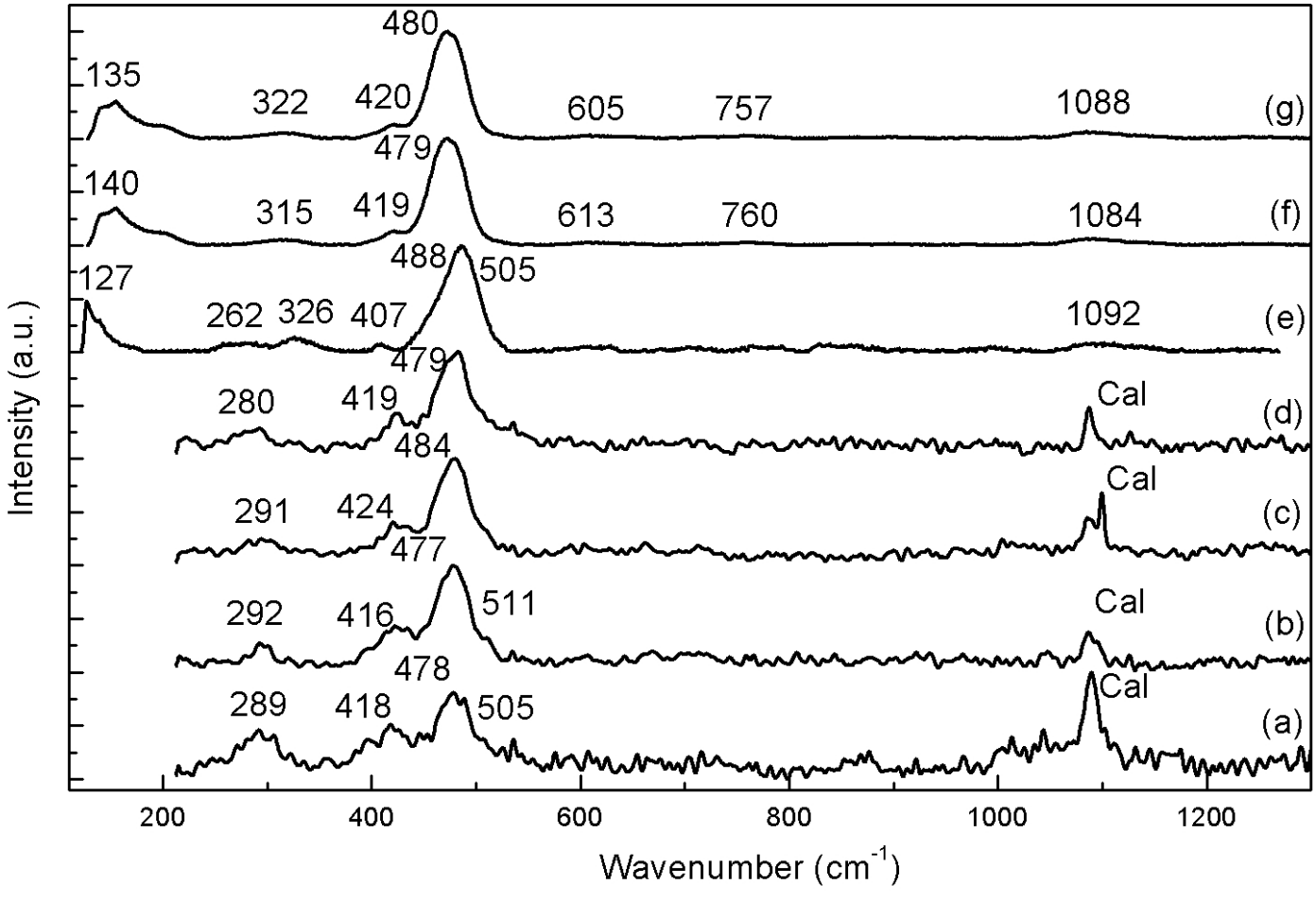
480
135
322
420
605
757
1088
(g)
479
140
315
419
613
760
1084
(f)
488
505
127
262
326
407
1092
(e)
479
280
419
Cal
(d)
484
Cal
291
424
(c)
477
Cal
292
416
511
(b)
478
Cal
289
418
505
(a)
Intensity (a.u.)
200
400
600
800
1000
1200
Wavenumber (cm-1)

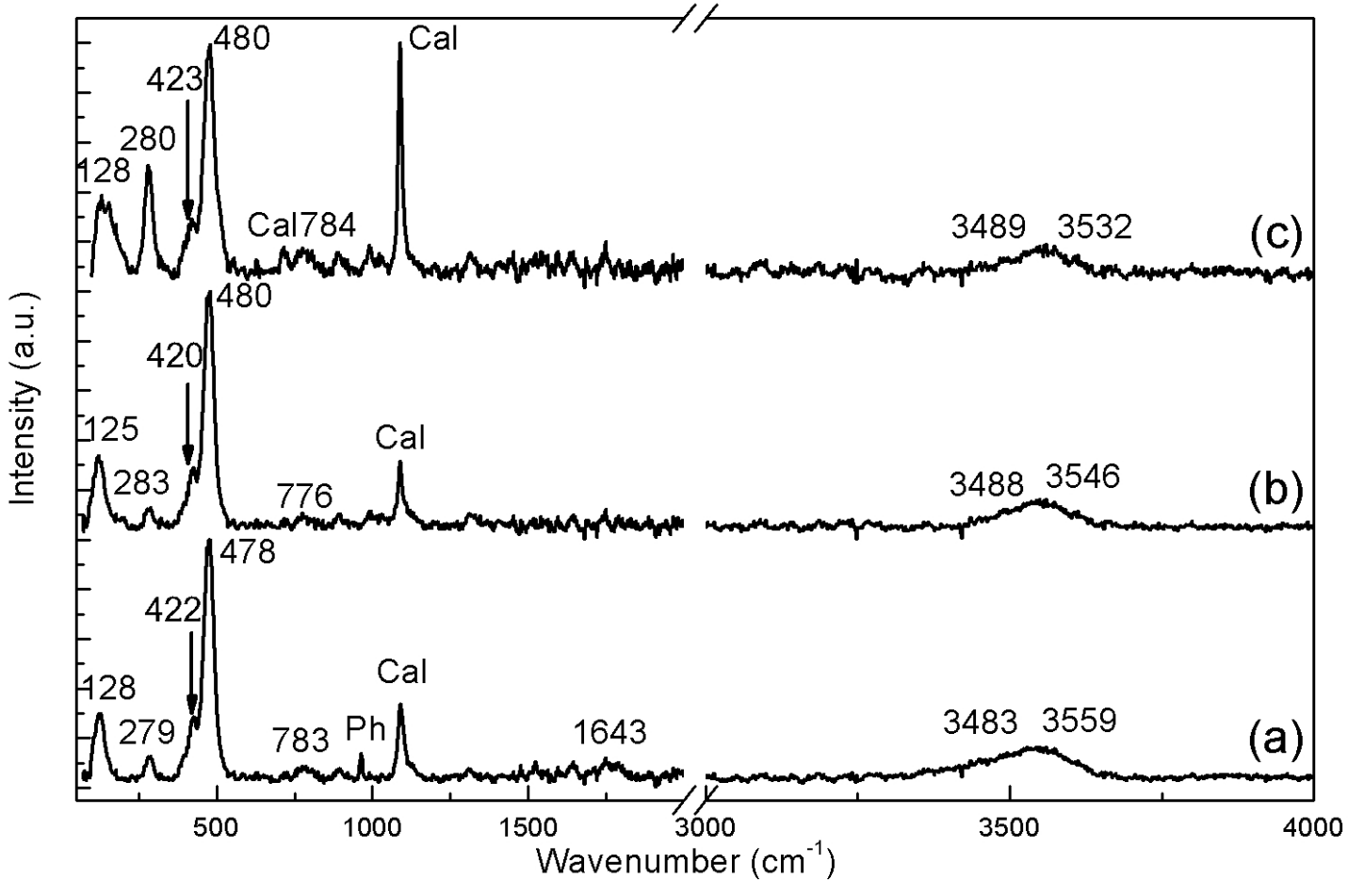
480
Cal
423
280
128
Cal784
3489
3532
(c)
480
420
125
Cal
283
776
3488
3546
(b)
478
422
128
Cal
279
783
Ph
1643
3483
3559
(a)
Intensity (a.u.)
500
1000
1500
3000
3500
4000
Wavenumber (cm-1)

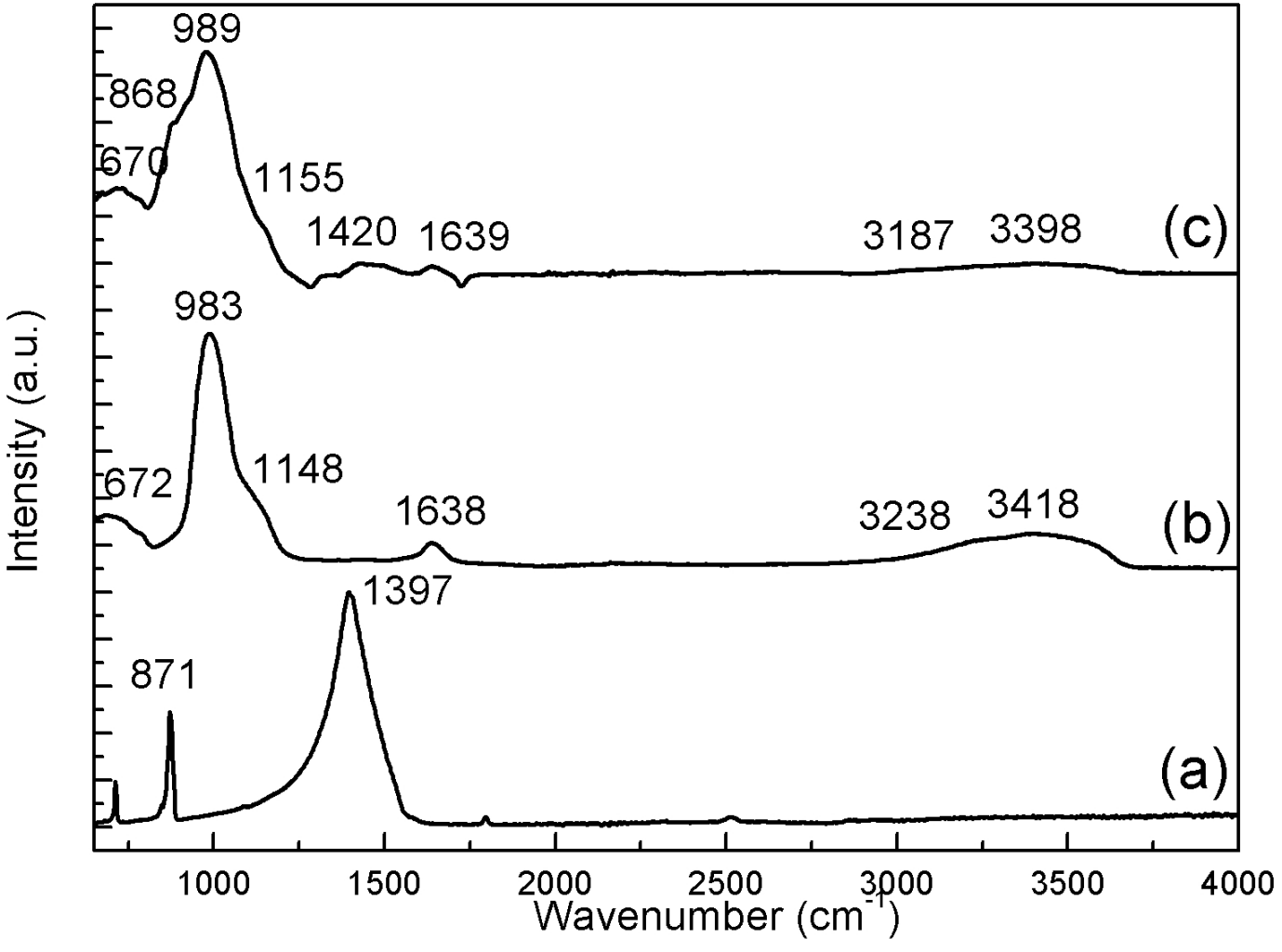
989
868
670
1155
1420
1639
3187
3398
(c)
983
672
1148
1638
3238
3418
(b)
1397
871
(a)
Intensity (a.u.)
1000
1500
2000
2500
3000
3500
4000
Wavenumber (cm-1)

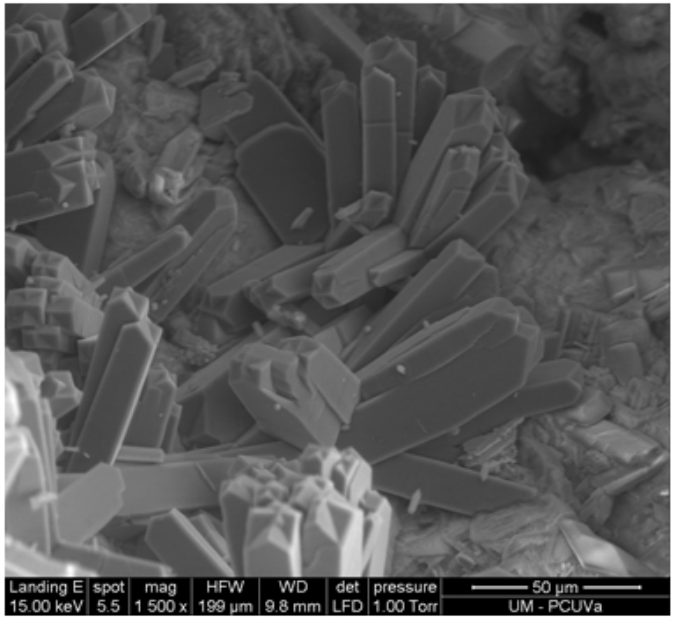
Landing E spot mag HFW WD det pressure 50 µm
15.00 keV 5.5 1 500 x 199 µm 9.8 mm LFD 1.00 Torr UM - PCUVa

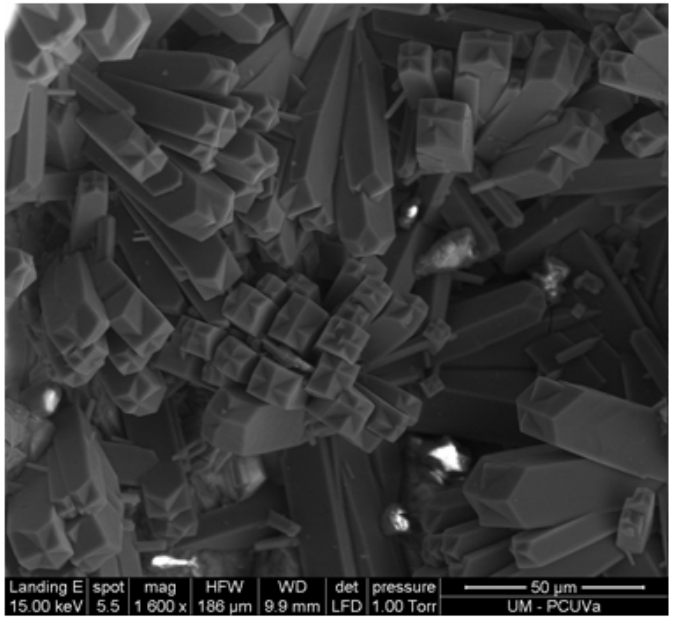
Landing E spot mag HFW WD det pressure 50 µm
15.00 keV 5.5 1 600 x 186 µm 9.9 mm LFD 1.00 Torr UM - PCUVa

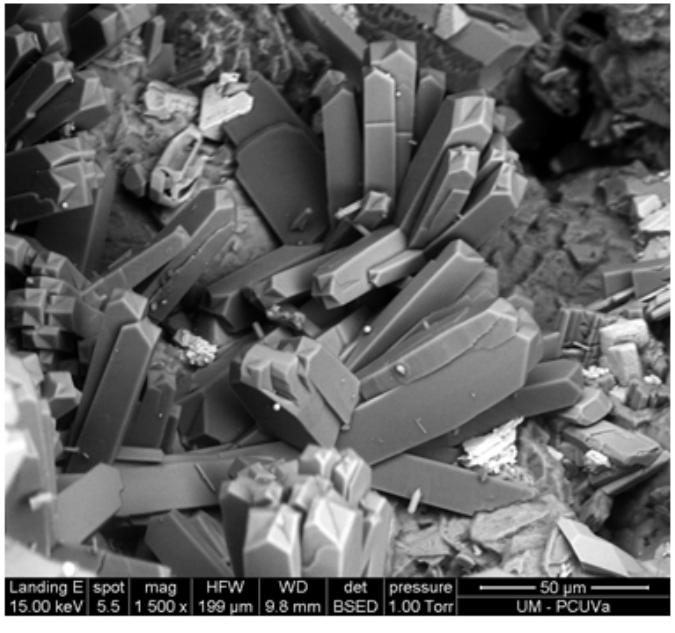
Landing E spot mag HFW WD det pressure 50 µm
15.00 keV 5.5 1 500 x 199 µm 9.8 mm BSED 1.00 Torr UM - PCUVa

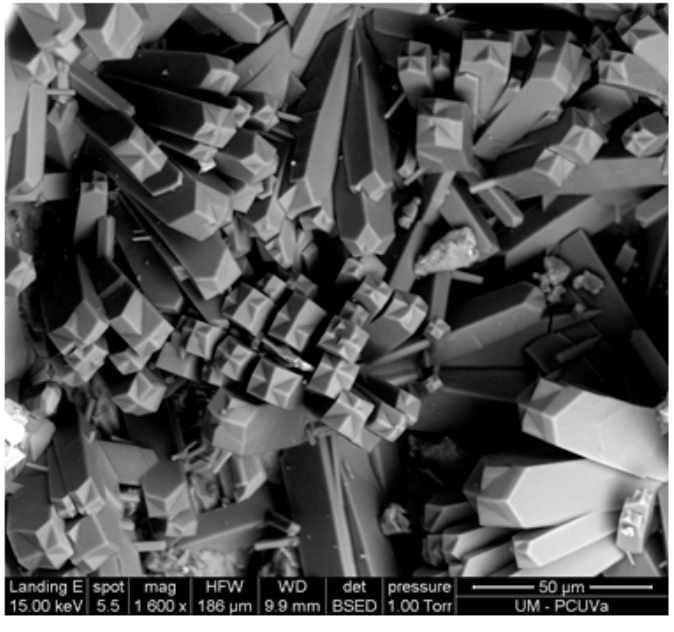
Landing E spot mag HFW WD det pressure 50 µm
15.00 keV 5.5 1 600 x 186 µm 9.9 mm BSED 1.00 Torr UM - PCUVa

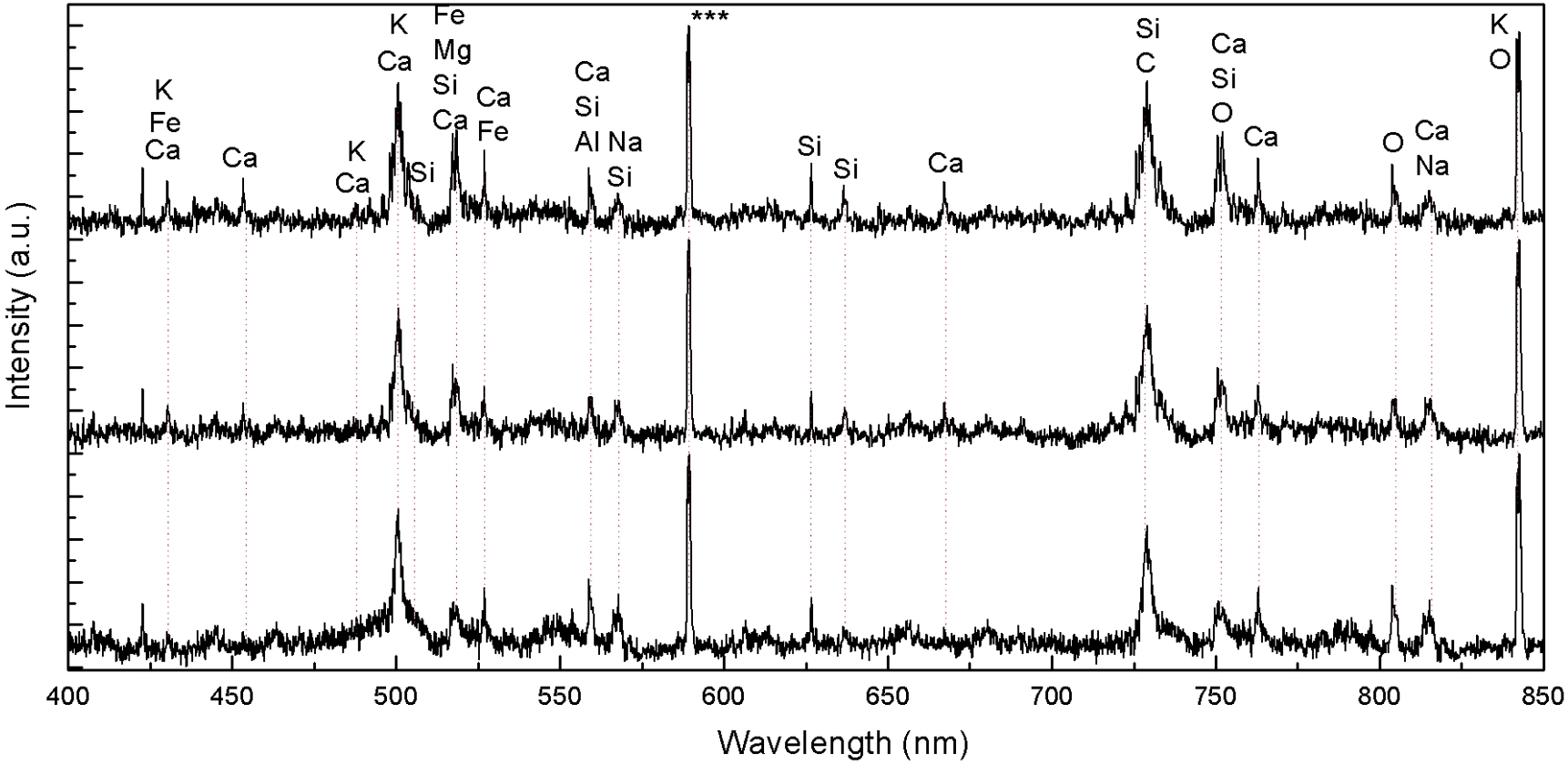
Intensity (a.u.)
Wavelength (nm)
400
450
500
550
600
650
700
750
800
850
K
Fe
Ca
Ca
K
Ca
K
Ca
Si
Fe
Mg
Si
Ca
Ca
Fe
Ca
Si
Al
Na
Si
***
Si
Si
Ca
Si
C
Ca
Si
O
Ca
O
Ca
Na
K
O

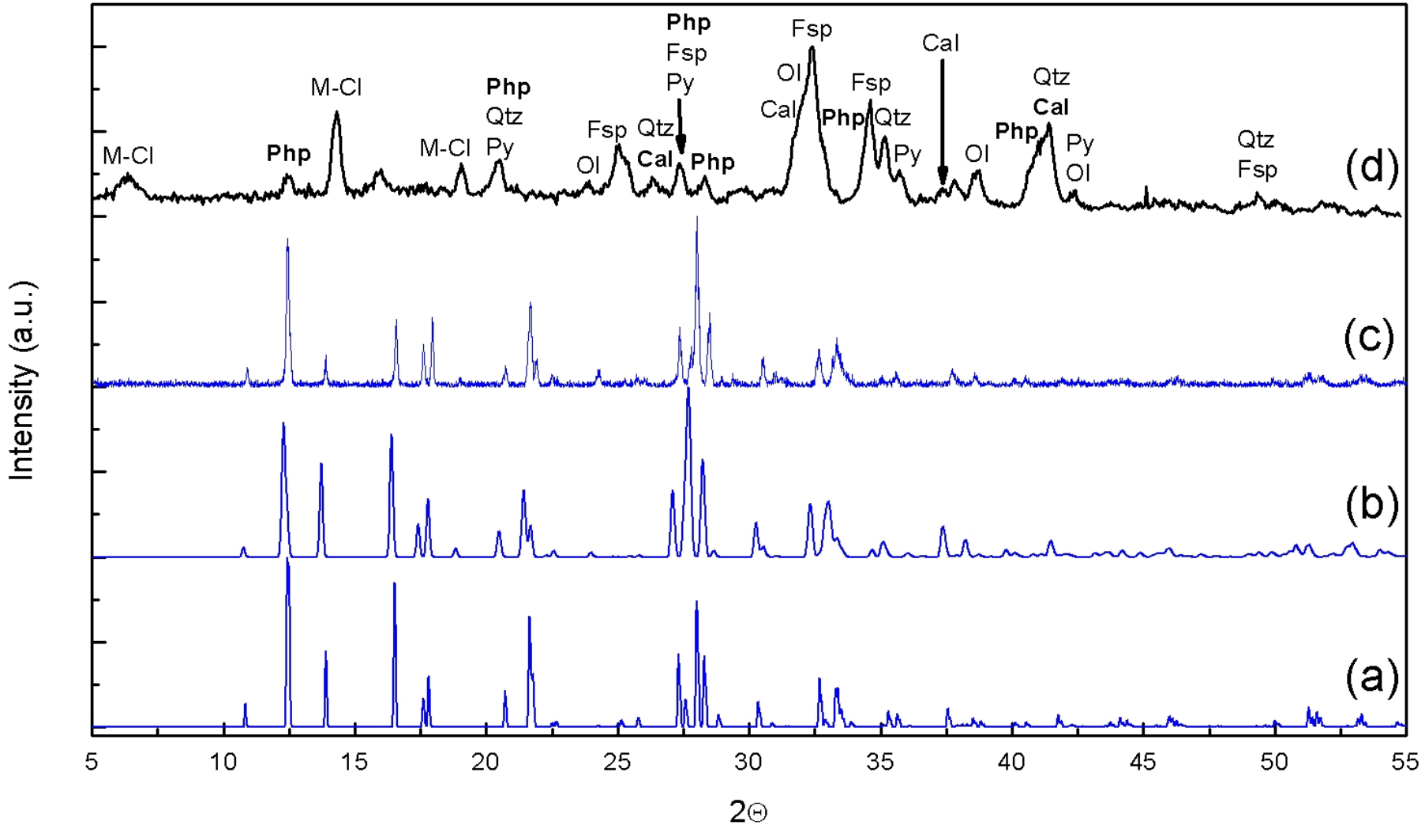
Intensity (a.u.)
M-Cl
Php
M-Cl
M-Cl
Php
Qtz
Py
Ol
Fsp
Qtz
Cal
Php
Php
Fsp
Py
Ol
Cal
Fsp
Php
Fsp
Qtz
Py
Cal
Ol
Php
Qtz
Cal
Py
Ol
Qtz
Fsp
(d)
(c)
(b)
(a)
5
10
15
20
25
30
35
40
45
50
55
2Θ

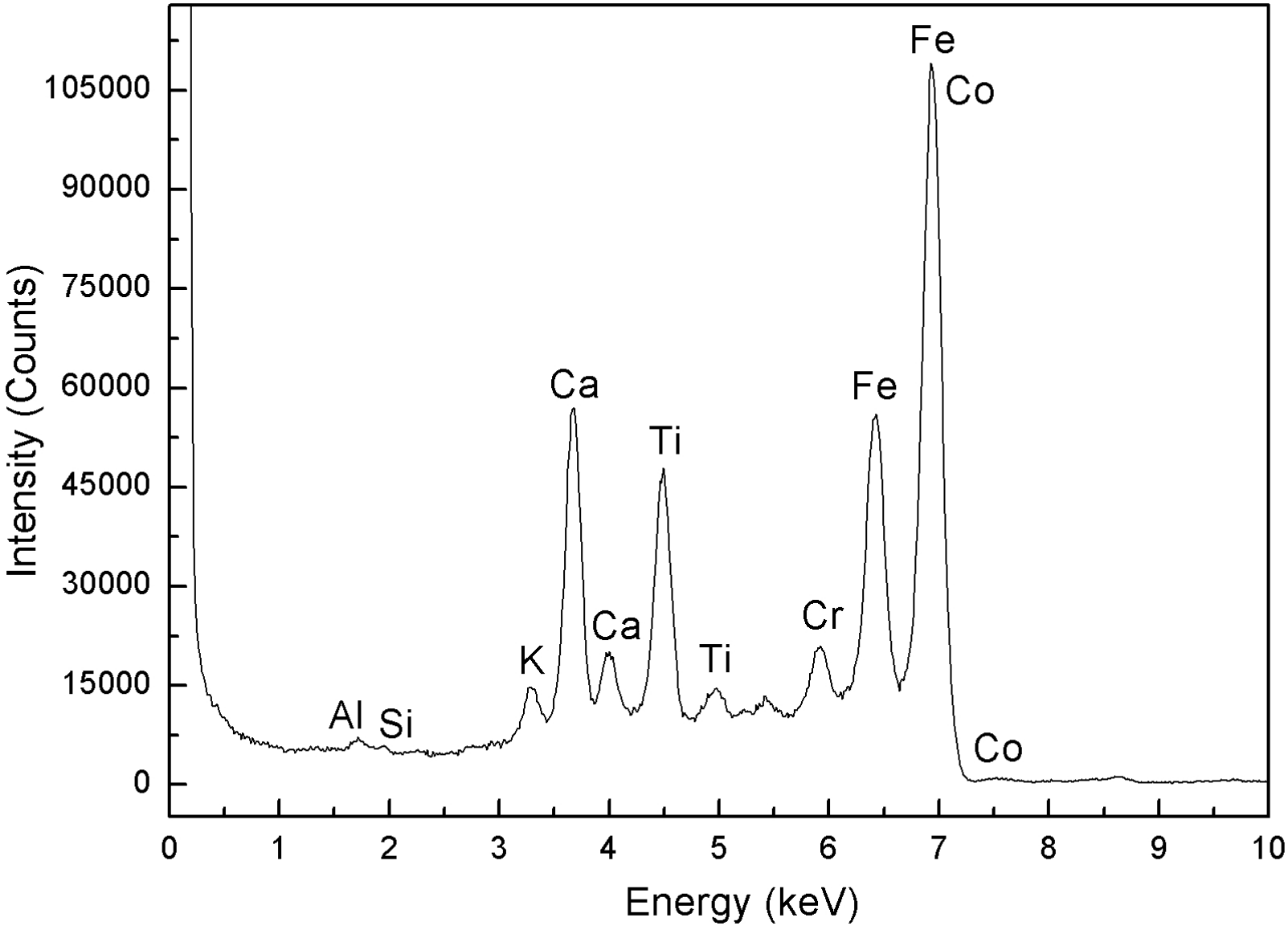
Intensity (Counts)
105000
90000
75000
60000
45000
30000
15000
0
0
1
2
3
4
5
6
7
8
9
10
Energy (keV)
Al
Si
K
Ca
Ca
Ti
Ti
Cr
Fe
Fe
Co
Co

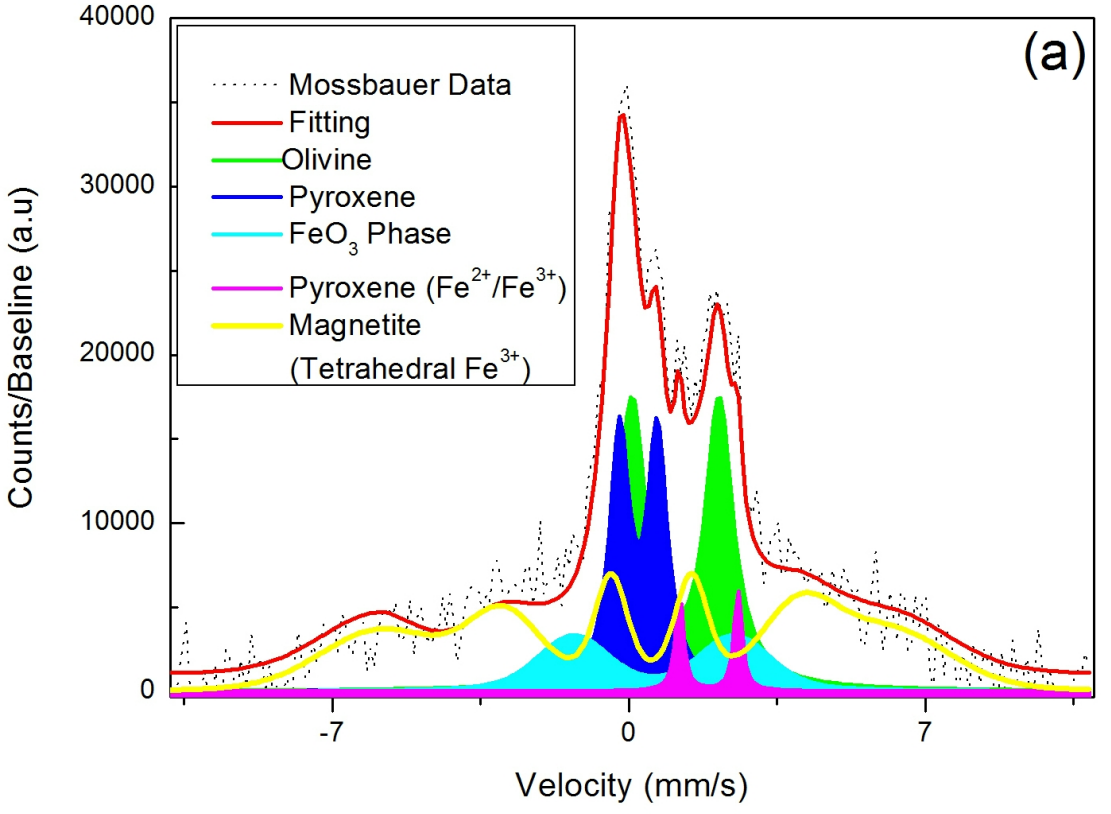
(a)
Mossbauer Data
Fitting
Olivine
Pyroxene
FeO3 Phase
Pyroxene (Fe2+/Fe3+)
Magnetite
(Tetrahedral Fe3+)
Counts/Baseline (a.u)
Velocity (mm/s)
40000
30000
20000
10000
0
-7
0
7

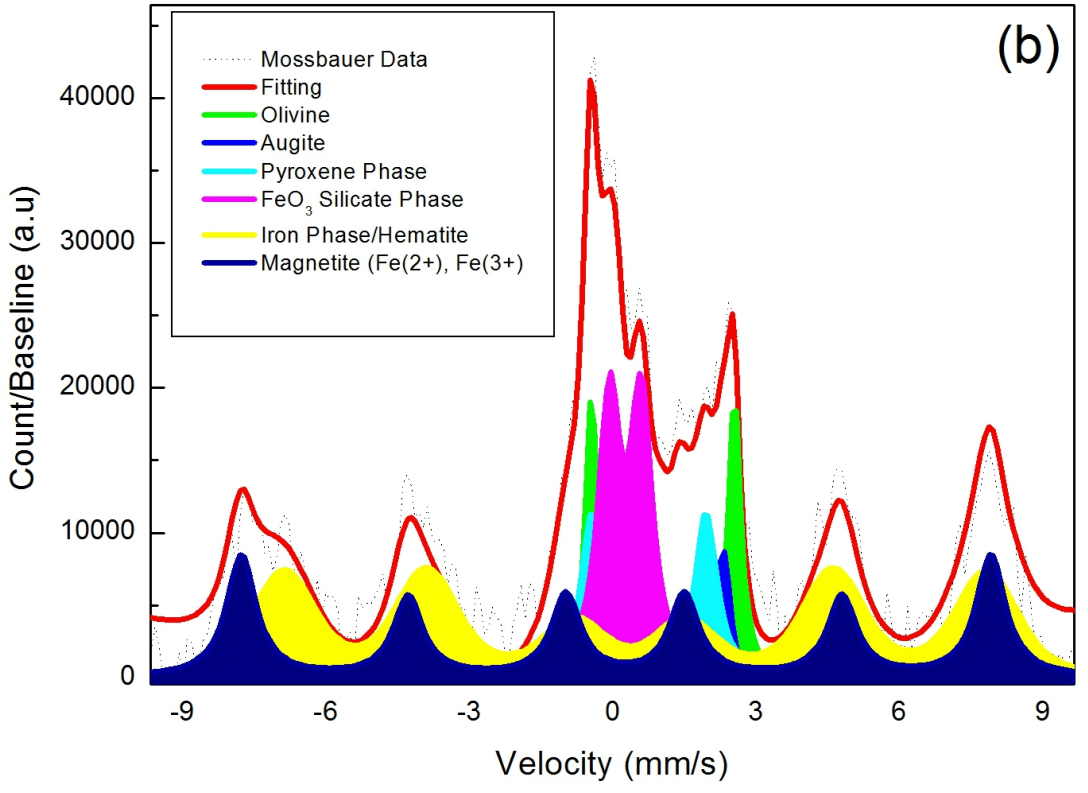
(b)
Mossbauer Data
Fitting
Olivine
Augite
Pyroxene Phase
FeO3 Silicate Phase
Iron Phase/Hematite
Magnetite (Fe(2+), Fe(3+)
Count/Baseline (a.u)
Velocity (mm/s)
40000
30000
20000
10000
0
-9
-6
-3
0
3
6
9

List of Tables

Table 1. Raman peak position (in cm^{-1}) of some selected spectra of the zeolite (phillipsite) in Las Arenas Negras volcano and RRUFF phillipsite from Figure 2. (**** = not possible to be assigned)

Spectra (a)	Spectra (b)	Spectra (c)	Spectra (d)	Ca-Phillipsite	Na-Phillipsite	K Phillipsite	Raman mode [21]	Raman mode [22]
				140	127	119	ν_{transl} (water), $\nu_{rotation}$ (water)	ν_{transl} (water) $\nu_{rotation}$(Si-Al)
					139	135	ν_{transl} (water), $\nu_{rotation}$ (water)	ν_{transl} (water) $\nu_{rotation}$(Si-Al)
				154	149	152	ν_{transl} (water), $\nu_{rotaition}$ (water)	****
				173		198	ν_{transl} (water), $\nu_{rotaition}$ (water)	ν_{transl} (water)
	218					210	****	ν_{transl} (water)
		267			262		****	
289	292	291	280		283	288	ν_{transl} (water), $\nu_{rotaition}$ (water)	****

307	300		298	315	326	307	$\nu_{twisting}$ (water)	$\nu_{libration}$ (water)
					330	322	$\nu_{twisting}$ (water)	****
					400		ν_{symm} O-(Al,Si)-O	$\nu_{libration}$ (water)
418	416	424	419	419	407	420	ν_{symm} O-(Al,Si)-O	$\nu_{libration}$ (water) $\nu_{libration}$ (Al,SiO_4)
	433		433				ν_{int} (Al,SiO_4)	ν_{int} (Al,SiO_4)
447	454			457	453		ν_{int} (Al,SiO_4)	ν_{int} (Al,SiO_4)
465	466	464	462	462		466	ν_{int} (Al,SiO_4)	****
		471		472	471		$\nu_{wagging}$ (water)	****
478	477		478	479		480	ν_{int} (Al,SiO_4)	ν_{int} (Al,SiO_4)
489	491	484	494	492	488	486	ν_{int} (Al,SiO_4)	ν_{int} (Al,SiO_4)
505	511				505		ν_{int} (Al,SiO_4)	ν_{int} (Al,SiO_4)
		523					ν_{int} (Al,SiO_4)	****
				613		605	ν_{int} (Al,SiO_4)	****
						642	$\nu_{rocking}$ (water)	ν_{int} (Al,SiO_4)

				760		757	ν_{symm}(Al,Si)-O	ν_{symm}(Al,Si)-O
1013							ν_{assym}(Al,Si)-O	ν_{int} (Al,SiO_4)
1044	1045		1076			1041	ν_{assym}(Al,Si)-O	ν_{assym}(Al,Si)-O
1089	**1986**	**1087**	**1084**	1084		1088	**Calcite**	ν_{assym}(Al,Si)-O **Calcite**
	1097	**1100**	**1090**		1092		**Calcite and Dolomite**	**Calcite and Dolomite**
			1110	1113	1133	1116	**Calcite and Dolomite**	**Calcite and Dolomite**
				1139		1248	****	****

Table 2. Raman peak position (in cm^{-1}) of some selected spectra of the zeolite (phillipsite) in Las Arenas Negras volcano from Figure 3 using the ESA-ExoMars RLS simulator from Figure 3.

Spectra (a)	Spectra (b)	Spectra (c)	Raman mode [21]	Raman mode [22]
102	103		ν_{transl} (water), $\nu_{rotaition}$ (water)	
114			ν_{transl} (water), $\nu_{rotaition}$ (water)	
128	125	128	ν_{transl} (water), $\nu_{rotaition}$ (water)	ν_{transl} (water) $\nu_{rotation}$(Si-Al)
		150		
		163		
279*	283*	280*	ν_{transl} (water), $\nu_{rotaition}$ (water) *Calcite	
291		294	****	
395		405	ν_{symm} O-(Al,Si)-O	$\nu_{libration}$ (water)
422	420	423	ν_{symm} O-(Al,Si)-O	$\nu_{libration}$ (water) $\nu_{libration}$ (Al,SiO_4)

449			ν_{int} (Al,SiO_4)	ν_{int} (Al,SiO_4)
466	464	465	ν_{int} (Al,SiO_4)	****
478	480	480	ν_{int} (Al,SiO_4)	ν_{int} (Al,SiO_4)
		507		ν_{int} (Al,SiO_4)
		718	Calcite	
783	776	784	ν_{symm}(Al,Si)-O	
892	893	890	****	
963			**Phosphate**	**Phosphate**
1088	1088	1087	**Calcite**	ν_{int} (Al,SiO_4) **Calcite**
1097	1105		**Calcite and dolomite**	ν_{assym}(Al,Si)-O Calcite and dolomite
1127			$\nu_{wagging}$ (water)	ν_{assym}(Al,Si)-O
1643			ν_{int} (Al,SiO_4)	
1750			****	
3483	3488	3489	ν_{assym} (O-H)	ν_{assym} (O-H)

3559	3546	3532	ν_{assym} (O-H)	ν_{assym} (O-H)
	3588	3570	ν_{assym} (O-H)	ν_{assym} (O-H)

Table 3. Mössbauer fitting parameters of the spectra in Figure 9 (a-b). IS: isomer shift; Γ: experimental line width and QS: quadrupole splitting parameter.

Sample	IS (mm/s)	QS (mm/s)	Γ (mm/s)	Ref
Fitting using Lorentzian line shapes with cosine smearing correction from Figure 9-(a)				
Olivine	0.98	2.06	0.40	[30,31]
Pyroxene	0.11	0.89	0.28	[30,31]
FeO_3 amorphous phase	1.77	1.39	0.11	[30,31]
Magnetite (Tetraderal)	0.22	11.97	3.79	[19,30,31]
Pyroxene ($Fe^{3+/2+}$)	0.48	3.79	0.39	[30,31]
Fitting using Lorentzian line shapes with cosine smearing correction from Figure 9-(b)				
Olivine	0.94	2.99	0.15	[30,31]
Augite	1.10	2.22	0.11	[30,31]
Fe-Silica phase	0.15	0.66	0.27	[30,31]
Amorphous iron phase	0.30	14.70	0.39	[30,31]
Magnetite (Octahedral)	0.55	15.56	0.38	[30,31]

Table 4. Comparison of the capabilities of the 7 systems employed in this investigation

Technique	Structural Identification	Elemental Composition	Geological Context	Penetration Capability
Raman Spectroscopy	Yes	Potencially (only major elements)	Yes (mapping)	No (only superficial)
Infrared Spectroscopy	Yes	No	Yes	No (only superficial)
XRD	Yes	No	Potentially	No (powdered samples)
XRF	No	Yes	No	No (Powdered samples)
LIBS	No	Yes	Yes (mapping)	Yes (few microns)
SEM-EDX	Yes (Imaging)	Yes	No	Yes
Mossbauer Spectroscopy	Yes (Fe mineral content)	No	Yes	Yes (few cms)

Table 5. Analytical techniques applied to the sample suite and their lab base and rover equivalents.

Experimental technique	**Laboratory Instrument**	**Twin Instrument used**	**ExoMars**	**MSL**	**MER**	**Mars 2020**
Raman Spectroscopy	Raman KOSI Holospec	RLS Simulator System	*RLS*	*****	*****	*SuperCam* *SHERLOC*
Infrared Spectroscopy	Bruker RSF 100/S	*****	*Micro Omega,* *ISEM*	*****	*Mini-TES*	****
LIBS	PortaLIBS 2000	*****	*****	*ChemCam*	*****	*SuperCam*
XRD/XRF	*****	Terra In-situ	*****	*CheMin*		*PIXL*
SEM-EDS	FEI - Quanta 200 FEG	*****	*****	*****	*****	*MastCam-Z*
Microscopic analysis	Nikkon SMZ 800	*****	*Clupi*	*****	*****	*MastCam-Z*
Mossbauer Spectroscopy	*****	Twin MIMOSII	*****	*****	*MIMOS II*	****

Supporting Materials

Table S-1. Summary of the documented mineral species detected in Las Arenas volcano, Tenerife, Canary Islands, Spain [13]. X indicates that these species were uniquely identified with the technique, while O indicates possible compatible results.

Minerals	**Raman**	**XRD**	**IR**
Magnetite (Fe_3O_4)	X	X	
Haematite (Fe_2O_3)	X	X	
Silica (SiO_2)	X	X	
Calcite ($CaCO_3$)	X		
Apatite ($Ca_5(PO4)_3(F,Cl,OH)$)	X		
Diopside ($MgCaSi_2O_6$)	X	X	O
Augite ($(Ca,Mg,Fe)_2(Si,Al)_2O_6$)	X	X	O
Forsterite ($(Fe,Mg)_2SiO_4$)	X	X	O
Anorthoclase ($(Na,K)AlSi_3O_8$)	X	O	O
Anorthite ($CaAl_2Si_2O_8$)		O	O
Albite($NaAlSi_3O_8$)	X	O	O
Oligoclase y Andesine $((Na,Ca)(Si,Al)_4O_8)$	X	O	O
Labradorite $((Ca,Na)(Si,Al)_4O_8)$		O	O

Phillipsite $((Ca,K,Na)_6(Si_{10}Al_6)O_{32}12H_2O)$	X		

Table S-2. IR band position (in cm^{-1}) of the selected spectra of the zeolite (phillipsite) in Las Arenas Negras volcano and RRUFF Ca-phillipsite from Figure 4.

IR Spectra	Ca-Phillipsite	Raman vibrational mode
670	672	ν_{sym}(Si-O-Al)
739	725	ν_{sym}(Si-O-Si)
786	777	
816	825	
868		Calcite
909	910	
	946	
989	983	ν_{asym}(Si-O-Si) and ν_{asym}(Si-O,Al)
1100	1071	
1155	1148	
1359		Calcite
1420		Calcite
1490		Calcite

1639	1638	ν(Al,Si)-OH
1682		ν(Al,Si)-OH
1700	1726	
3187	3238	H_2O
3398	3418	ν_{assym} (O-H)
3554	3556	ν_{assym} (O-H)

Table S-3. Elemental composition of the 4 different vesicles presented in Figure 1.

%Oxygen	Point (a)	Point (b)	Point (c)	Point(d)
CO	04.33	07.71	15.90	11.87
Na_2O	06.21	05.15	04.66	05.89
MgO	01.02	02.20	02.23	00.94
Al_2O_3	21.16	18.24	17.55	21.86
SiO_2	52.41	45.50	42.18	48.39
K_2O	06.28	01.81	03.87	03.14
P_2O_5	*****	*****	0.71	*****
CaO	04.08	06.63	09.99	03.80
TiO_2	00.85	01.55	01.35	00.68
FeO	03.66	10.21	01.46	03.43